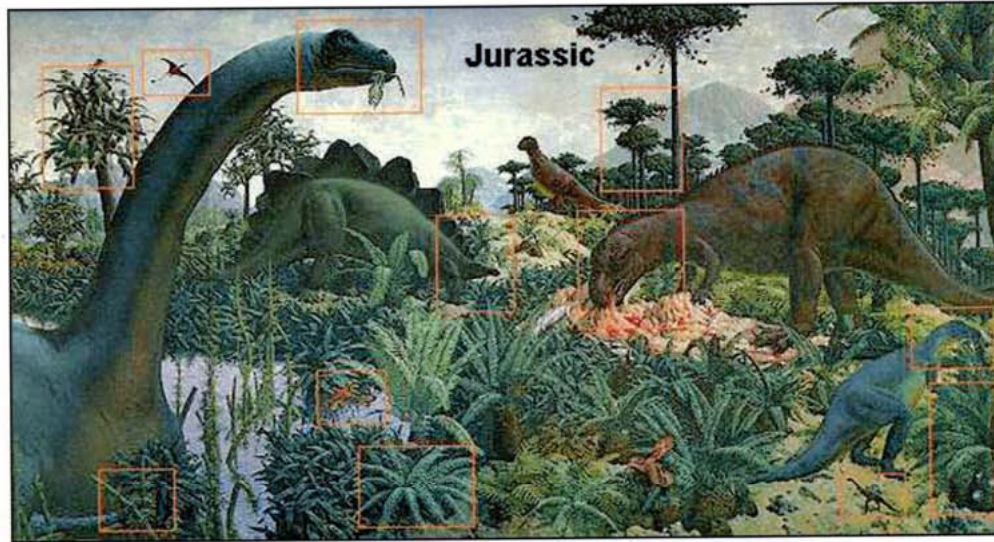
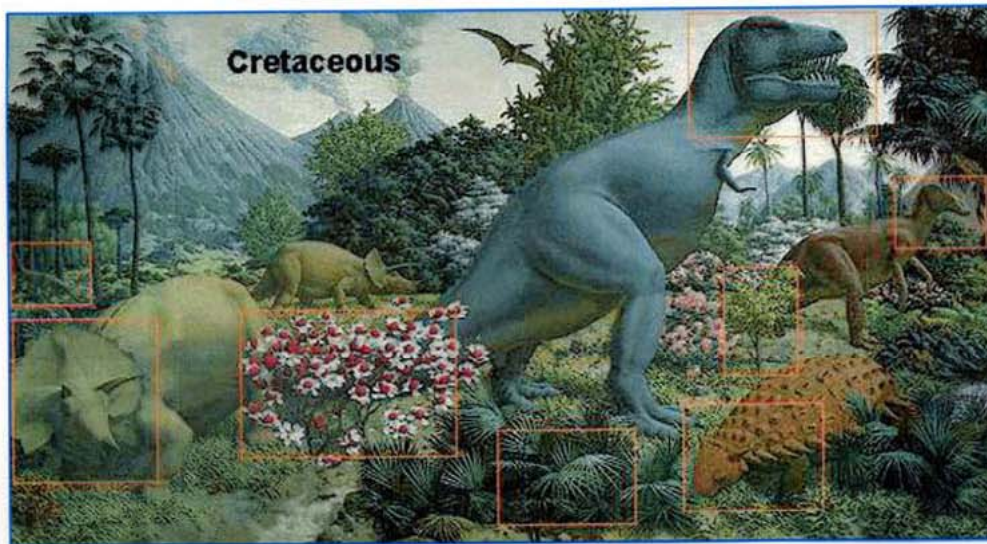


Mesozoic Warmth



Jurassic 220-140 Ma

Cretaceous 140-65 Ma



- Ferns & alligators in Siberia
- Dinosaur bones in AK (N of Arctic Circle)



Stanley (2000)

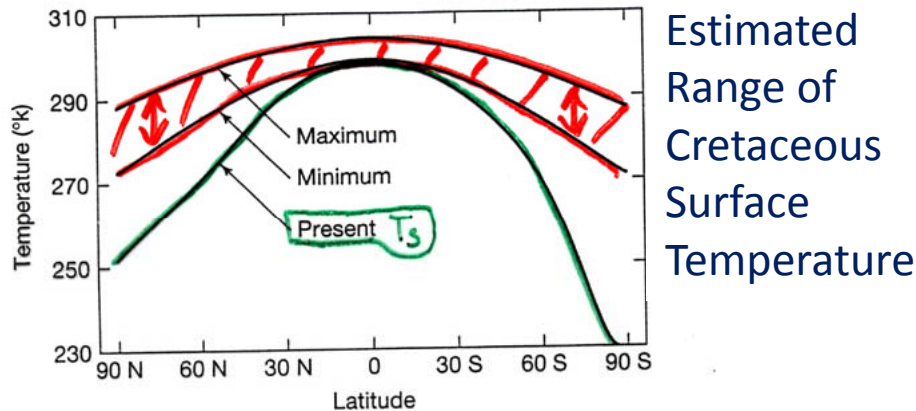
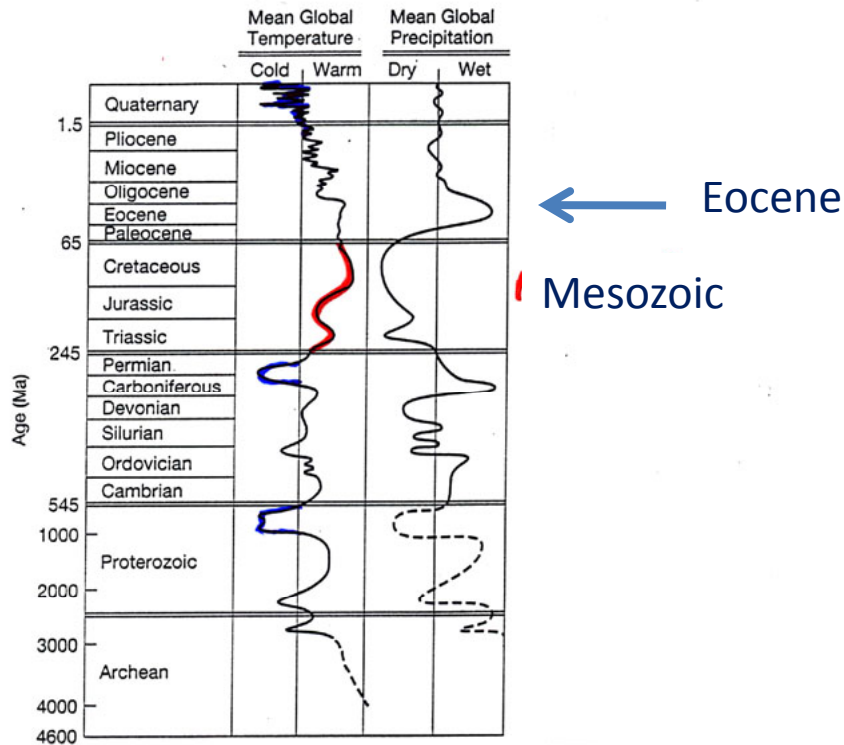


FIGURE 8-15

Estimated limits on longitudinally averaged surface temperatures during the mid-Cretaceous period, 100 m.y. ago, as compared with today. (After E. J. Barron and W. M. Washington, "The Carbon Cycle and Atmospheric CO₂," *Geophysical Monograph* 32, AGU, Washington, D.C., 1985.)

20°-50° Warmer at Poles!

2°-6° Warmer at Equator

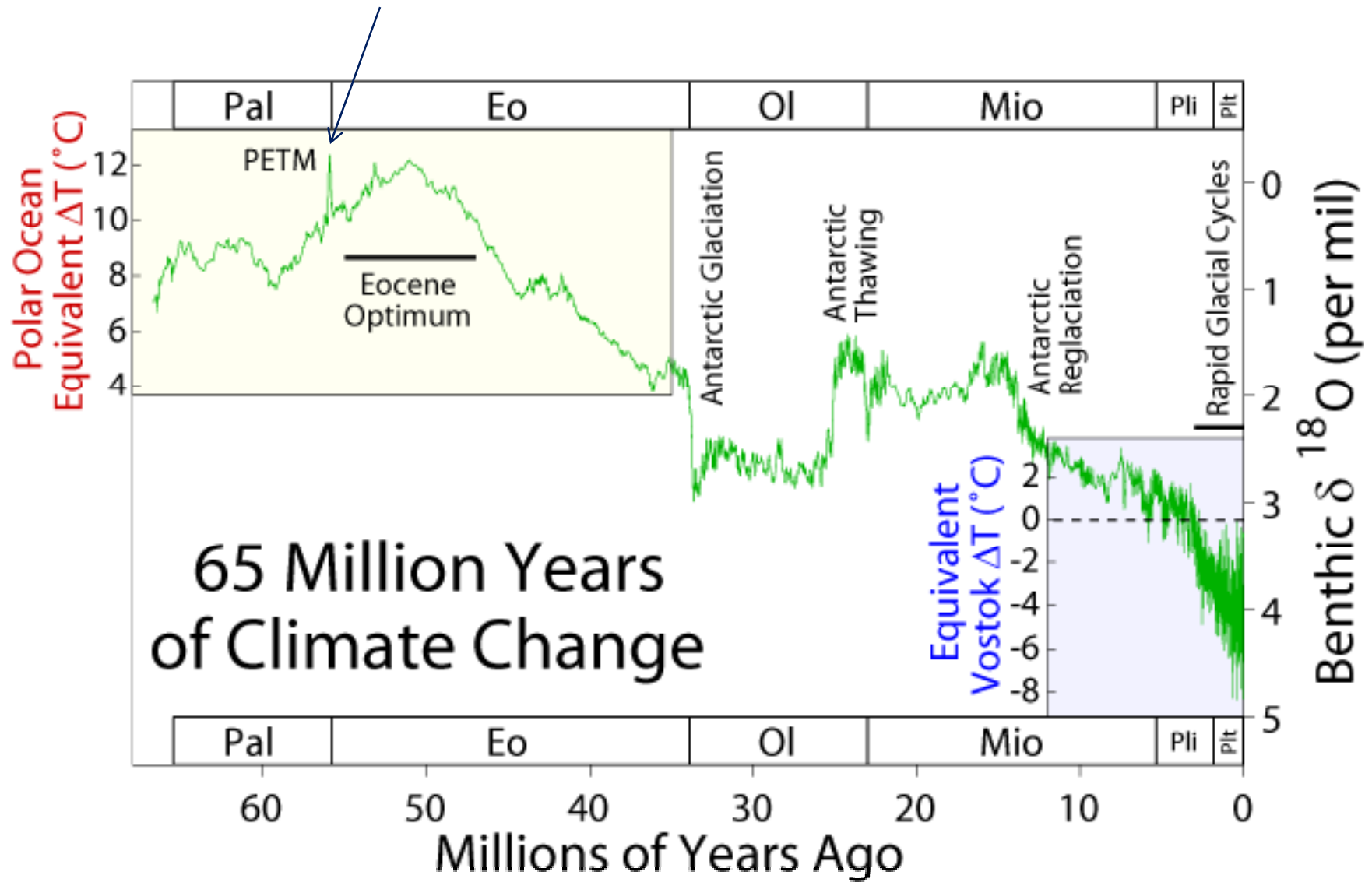
Decreased Equator-to-Pole Temperature Gradient

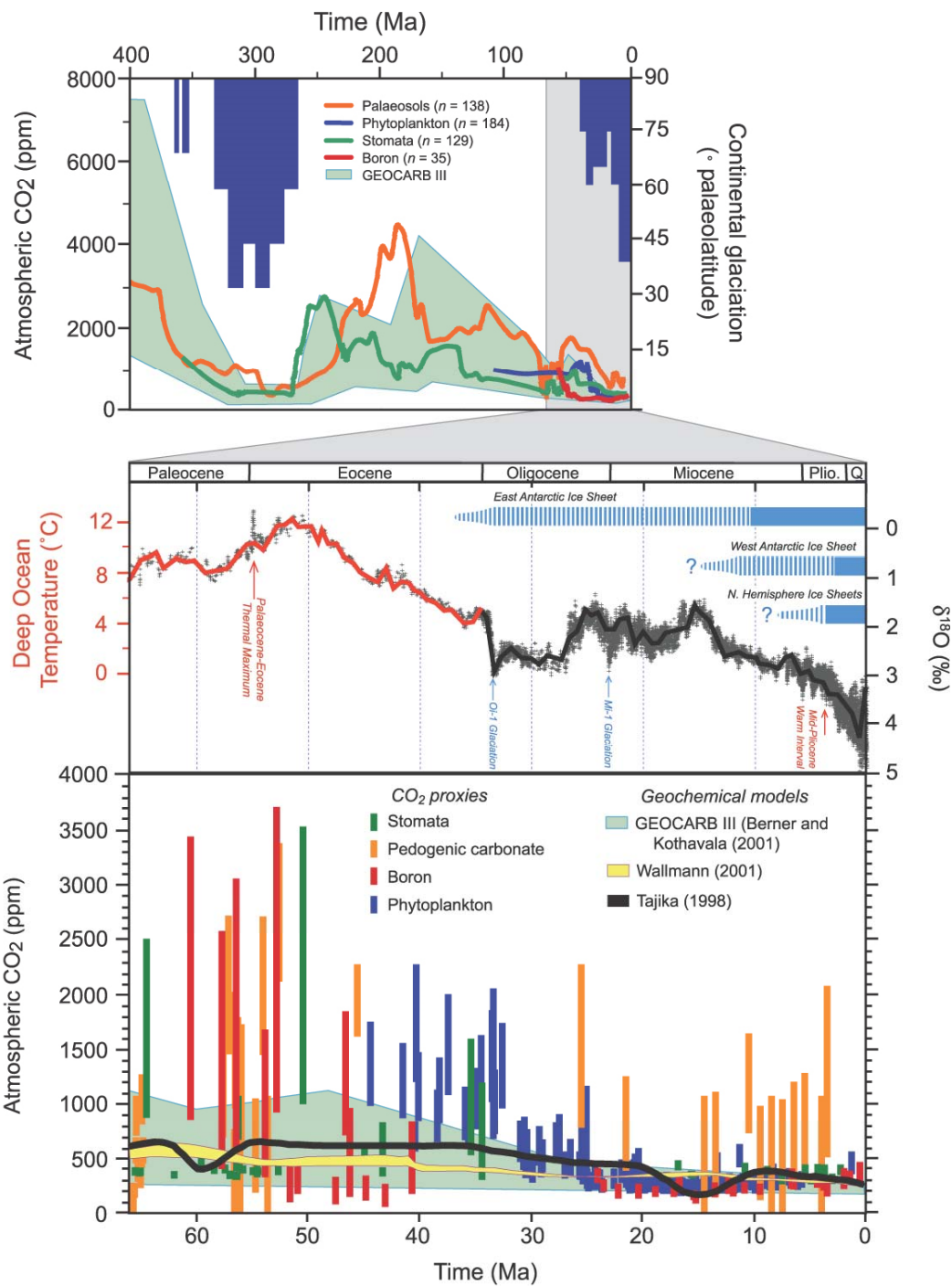
Kump et al. (1999)

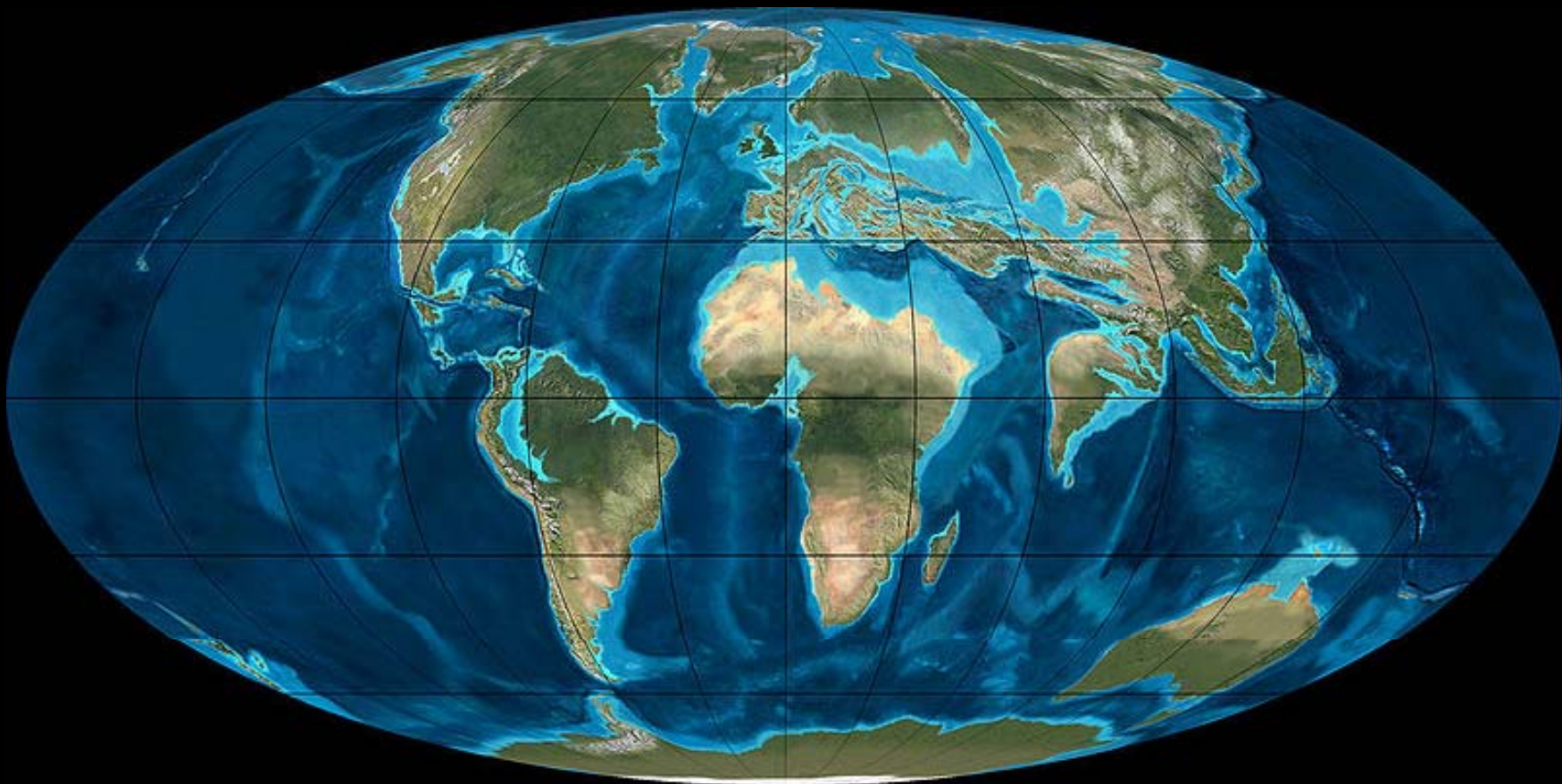
Warm Climates: The Eocene

65 -34 Ma


Paleocene-Eocene Thermal Maximum








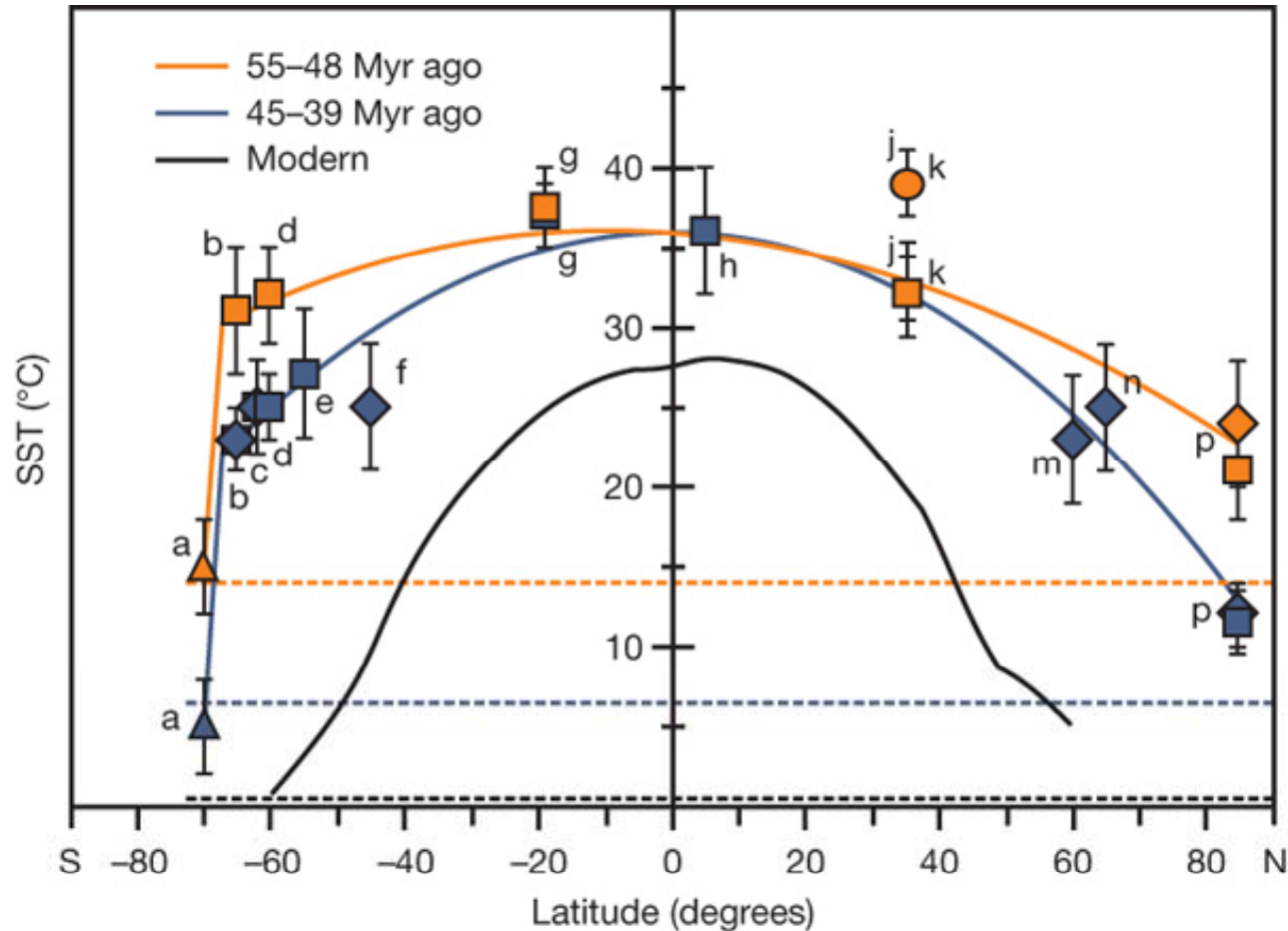


 Jahren AH. 2007.
Annu. Rev. Earth Planet. Sci. 35:509–40



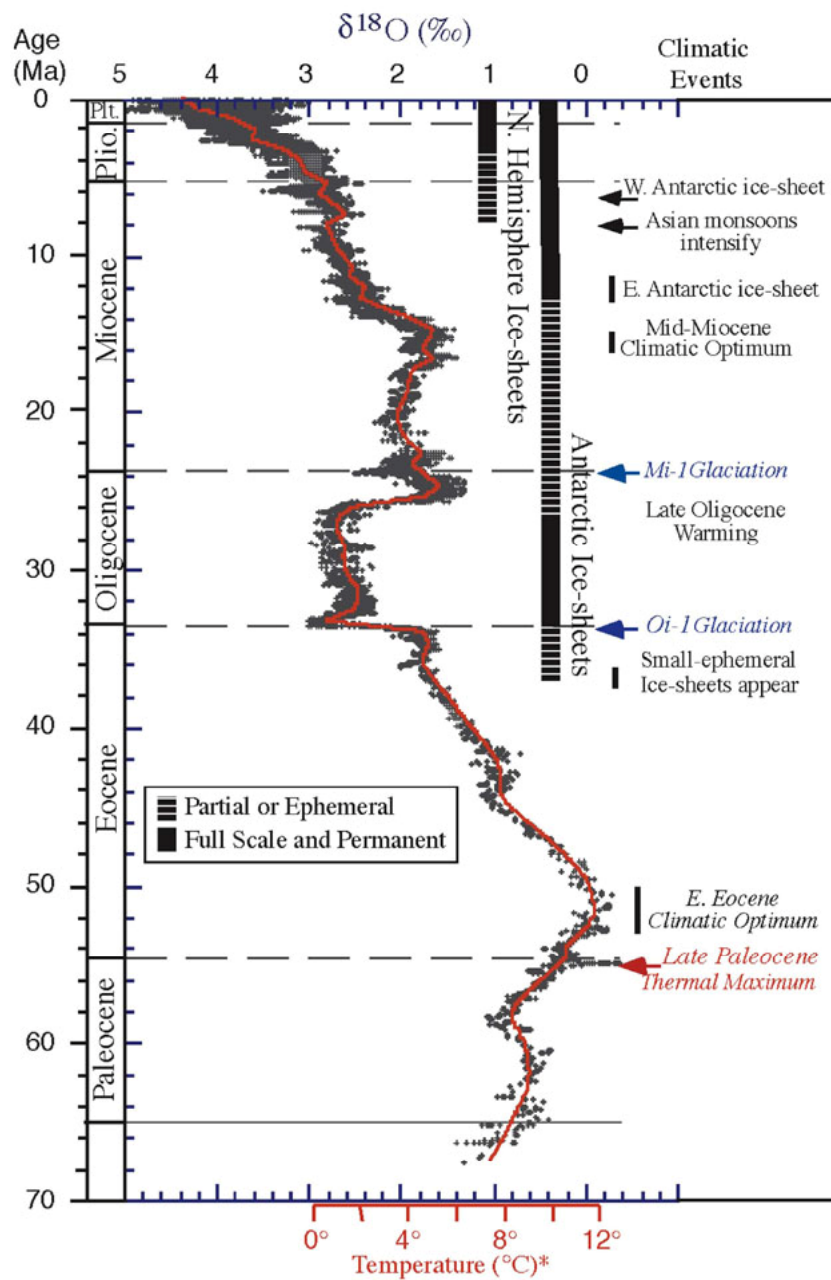
 Jahren AH. 2007.
Annu. Rev. Earth Planet. Sci. 35:509–40

Early and Middle Eocene latitudinal SST gradients.



Bivalve-shell ^{18}O (triangles), TEX_{86} (squares) and (diamonds) SST reconstructions for the Early (orange) and mid-Middle (blue) Eocene. Data are from Seymour Island¹⁸ (a), the East Tasman Plateau (b), Deep Sea Drilling Project (DSDP) Site 277⁹ (c), New Zealand^{15,16} (d), DSDP Site 511⁹ (e), ODP Site 1090⁹ (f), Tanzania¹ (g), ODP Site 925⁹ (h), New Jersey³ (j, k; circle represents peak PETM SSTs³), ODP Site 336⁹ (m), ODP Site 913⁹ (n) and the Arctic Ocean^{2,28,29} (p) ([Supplementary Fig. 1](#)). Error bars indicate the range of variation. Gradients represent second-order polynomials, excluding bivalve-shell data. Black and dashed lines represent the present-day zonally averaged latitudinal temperature gradient³⁰ and age-specific deep-sea temperatures, respectively

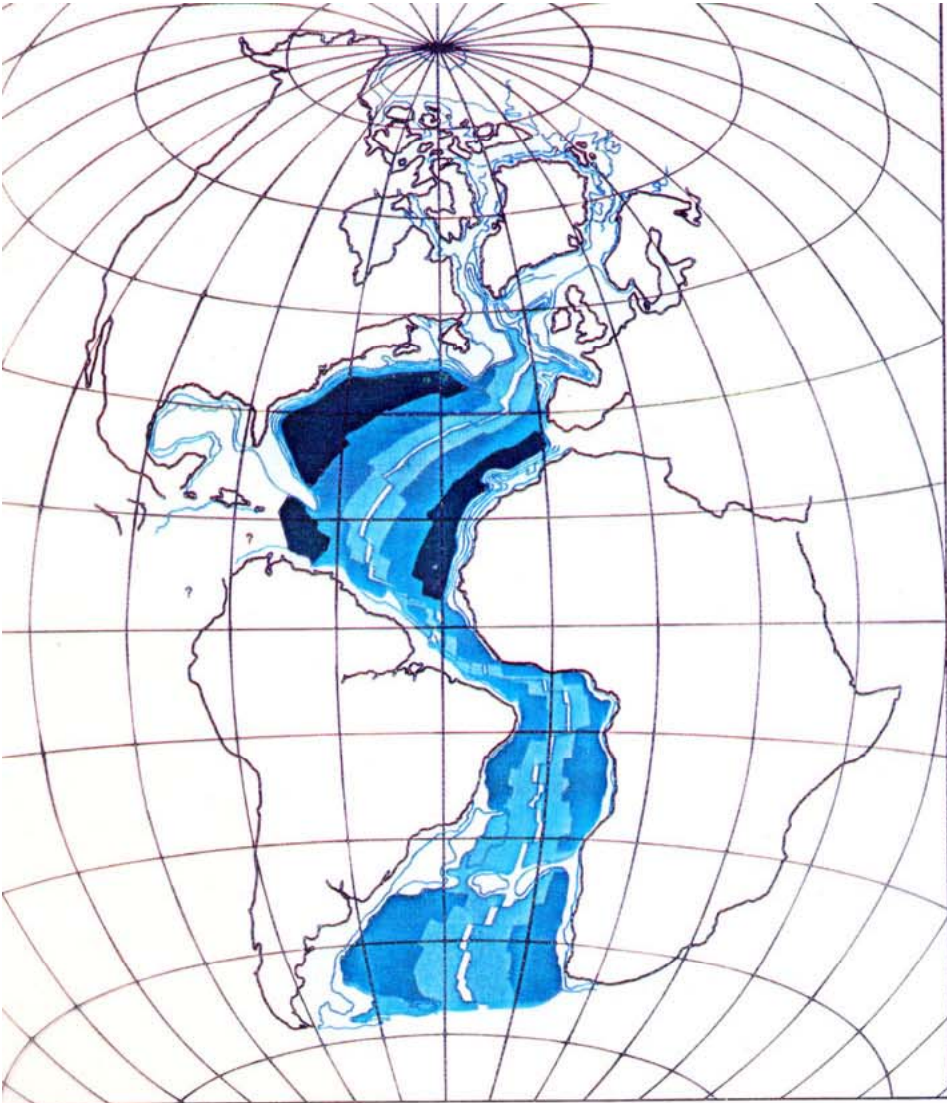
Cenozoic Benthic O18



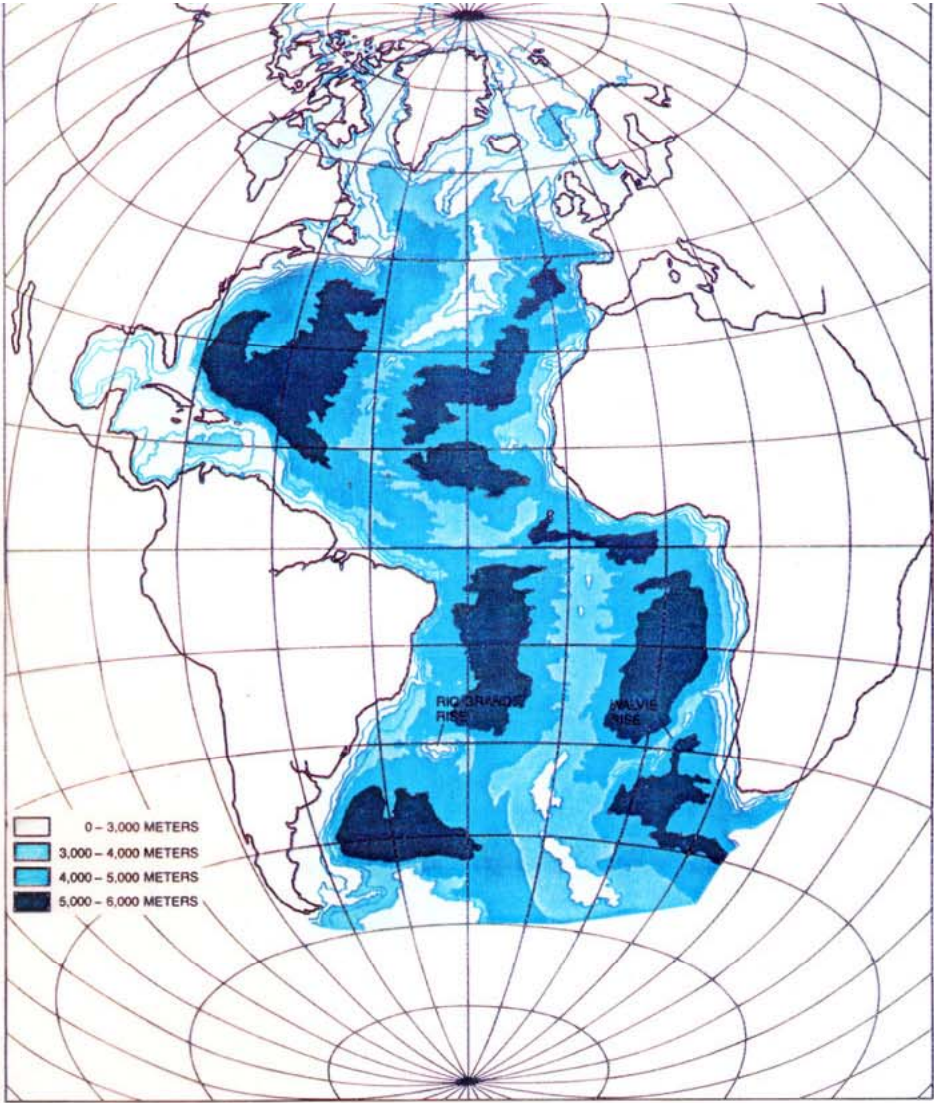
Cenozoic Cooling 80-0 Ma

Why?

Changing continental configuration and ocean basins

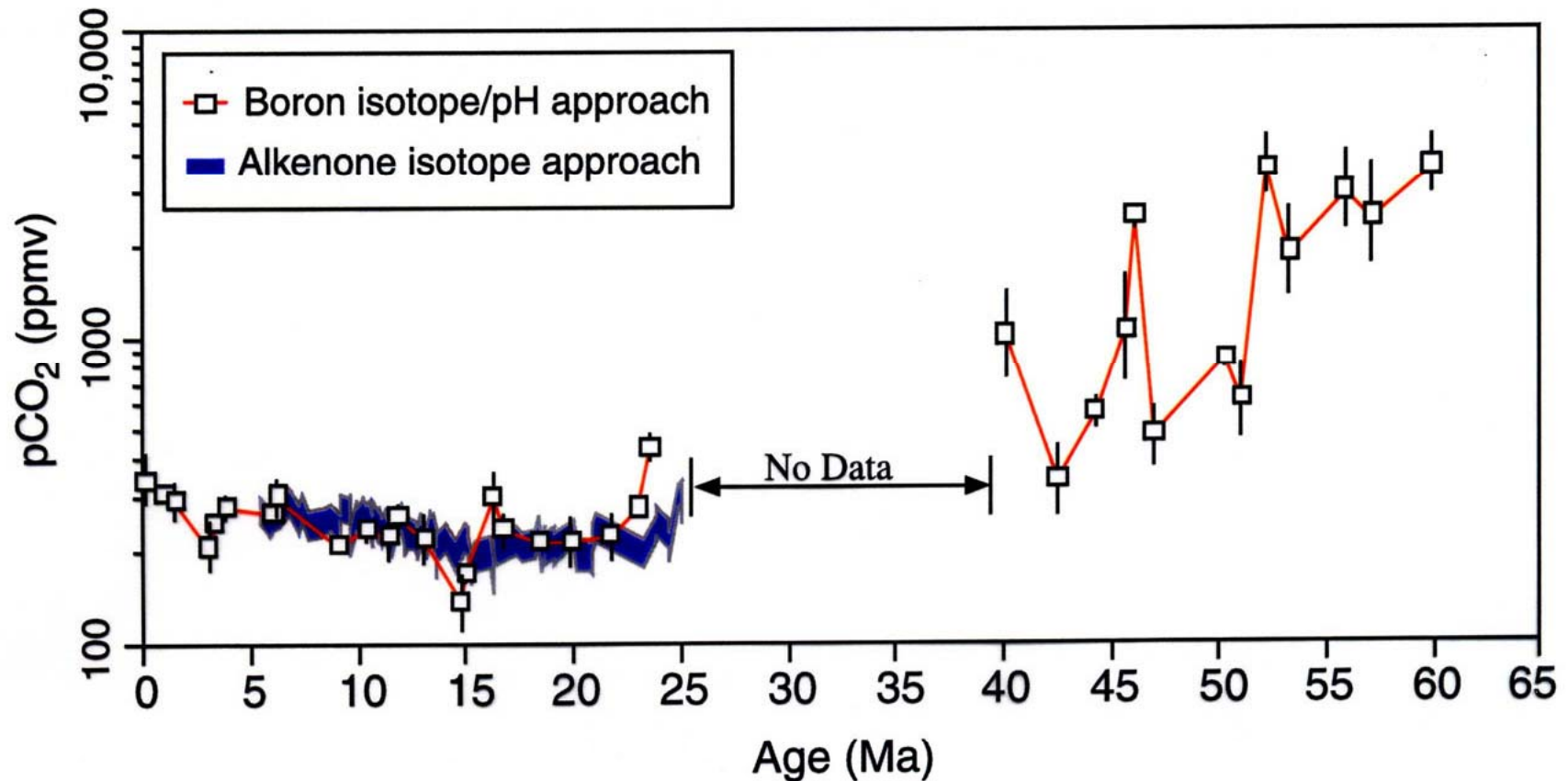


80 million years ago



Today

Boron Isotopes in Seawater Also Indicate Large Cenozoic CO₂ Decline

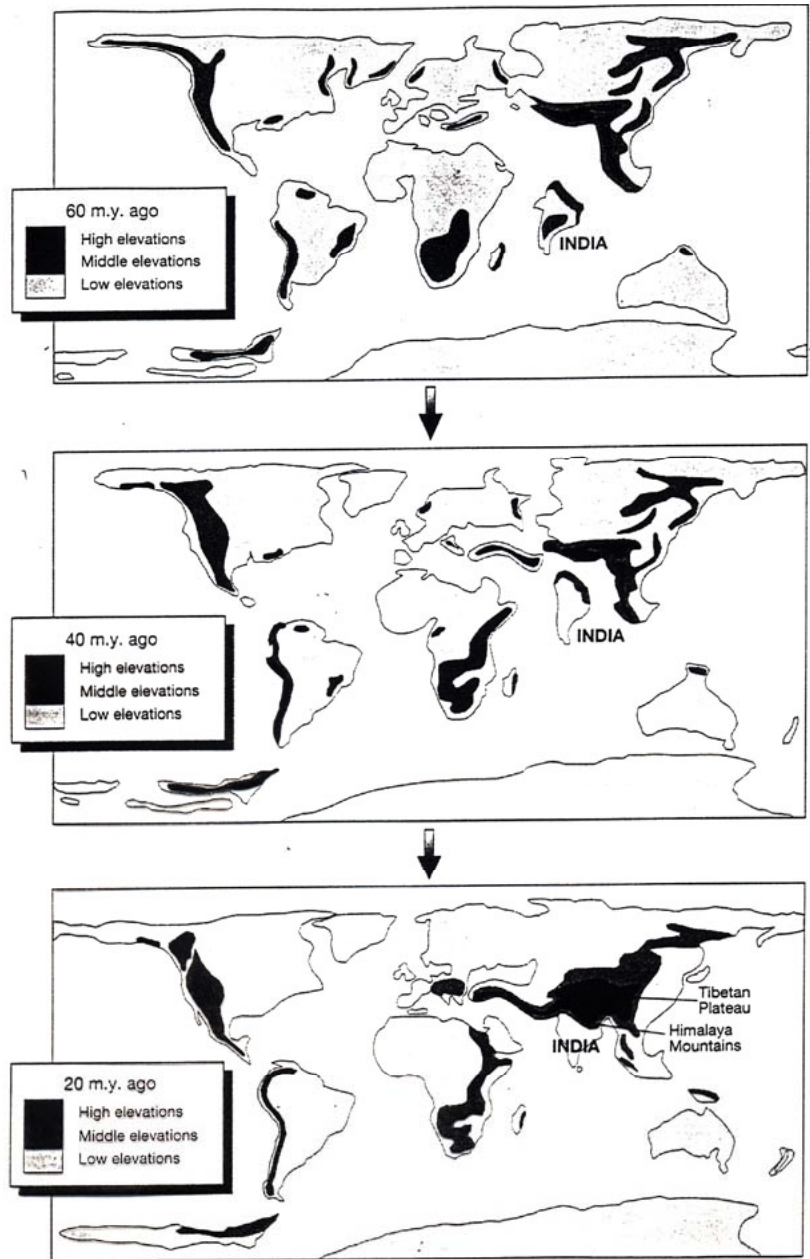


$$\delta^{11}\text{B} = \left[\frac{(^{11}\text{B}/^{10}\text{B})_{\text{smp}}}{(^{11}\text{B}/^{10}\text{B})_{\text{std}}} - 1 \right] \times 1000\text{‰}$$

- B in seawater: $\text{B}(\text{OH})_3$, $\text{B}(\text{OH})_4^-$
- Relative abundance controlled by pH
- B incorporated into calcite: $\text{B}(\text{OH})_4^-$
- Strong isotopic fractionation between ^{10}B & ^{11}B :
 ^{10}B = tetrahedral coordination, -19.8‰ relative to ^{11}B

in Zachos et al. (2001)

Himalayan Orogeny/Tibetan Plateau Uplift



60 Ma

40 Ma

20 Ma

Link to Himalayan Orogeny & Uplift of Tibetan Plateau? (Raymo and Ruddiman, *Nature*, 1992)

Catastrophic Climate Change

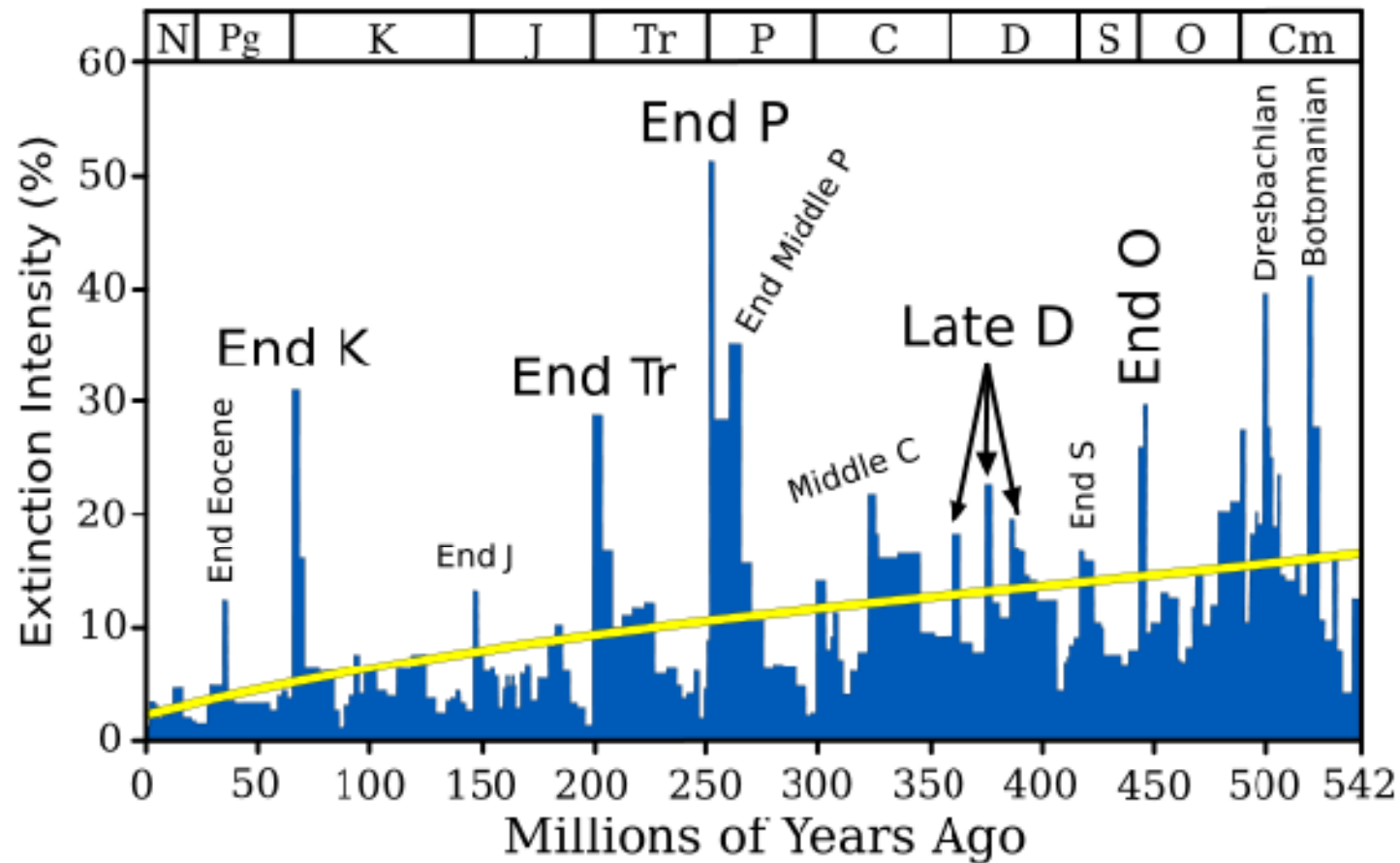


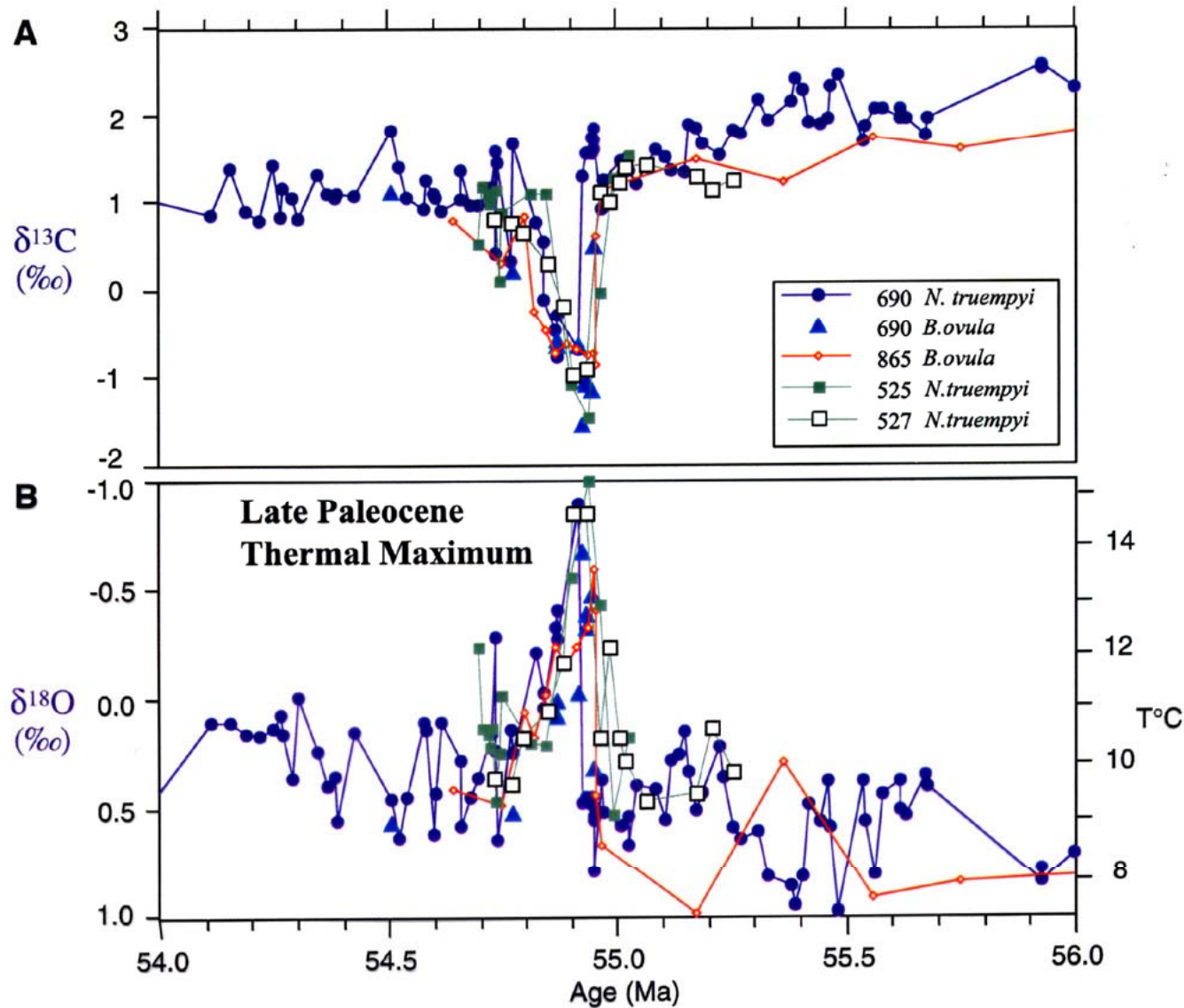
—DON
DAVIS—

D.DAVIS

Mass Extinctions of Species

Marine Genus Biodiversity: Extinction Intensity





Did a Gas Hydrate Release of Methane (2600 Gt) caused Late Paleocene Thermal Maximum?

Benthic foraminifera from Atlantic & Pacific

- CO_2 not the only greenhouse gas we need to consider when evaluating warm episodes.

Zachos et al. (2001)

Bolide Impacts

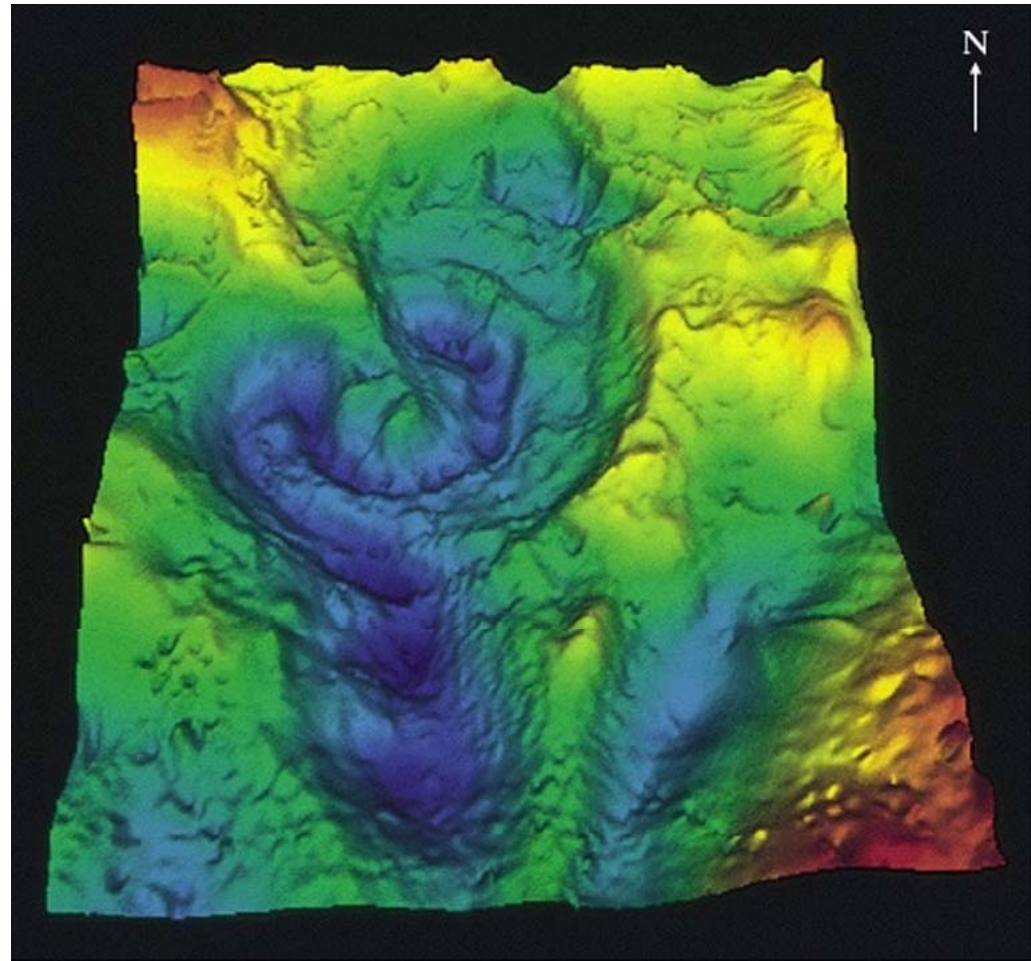
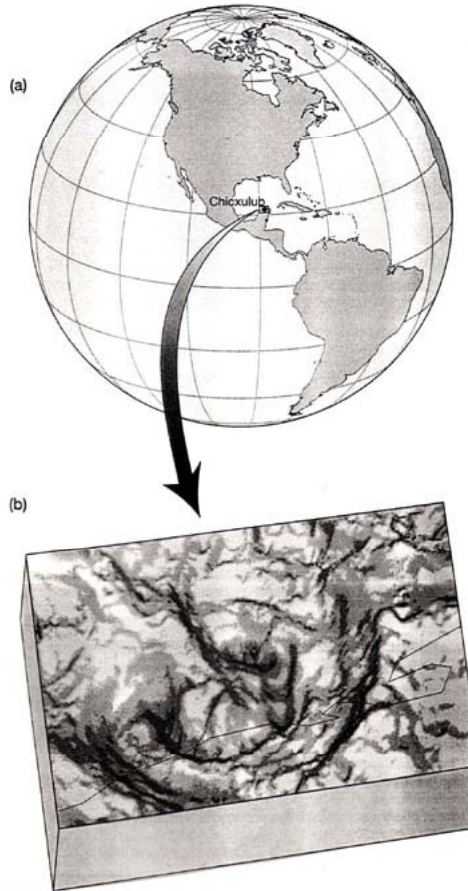


- Impacts large enough to influence climate every ~30 million years
- Climate cooling owing to stratospheric aerosols
- Short-term extreme heating by re-entrant debris
- Destruction of stratospheric ozone through massive injections of water
- Acid rain

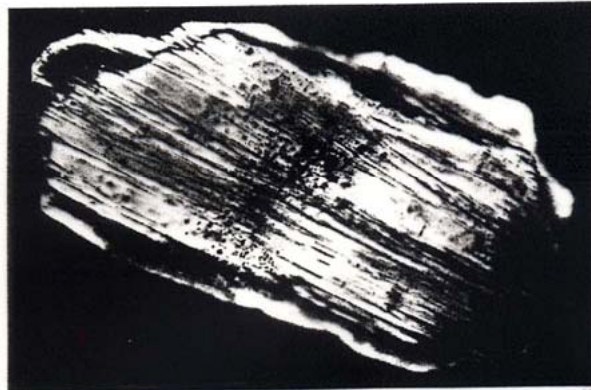
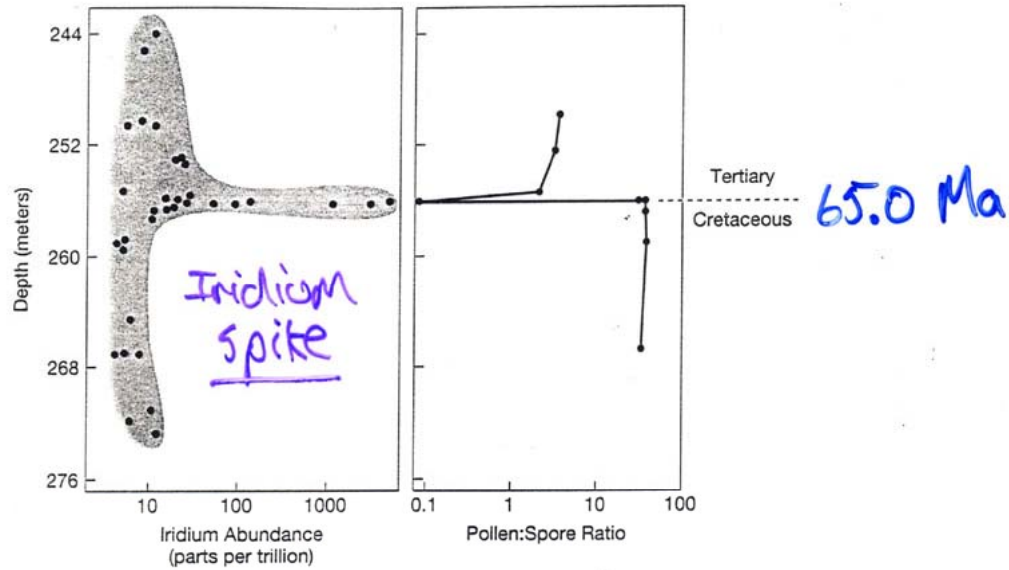
Chicxulub Crater Gulf of Mexico

- 200 km crater
- 10-km impactor
- 65 Myr BP
- Extinction of 75% of all species!

K-T Impact Crater

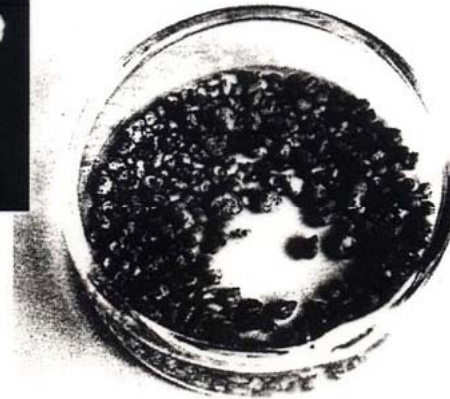


Evidence for Meteorite Impact @ K-T Boundary



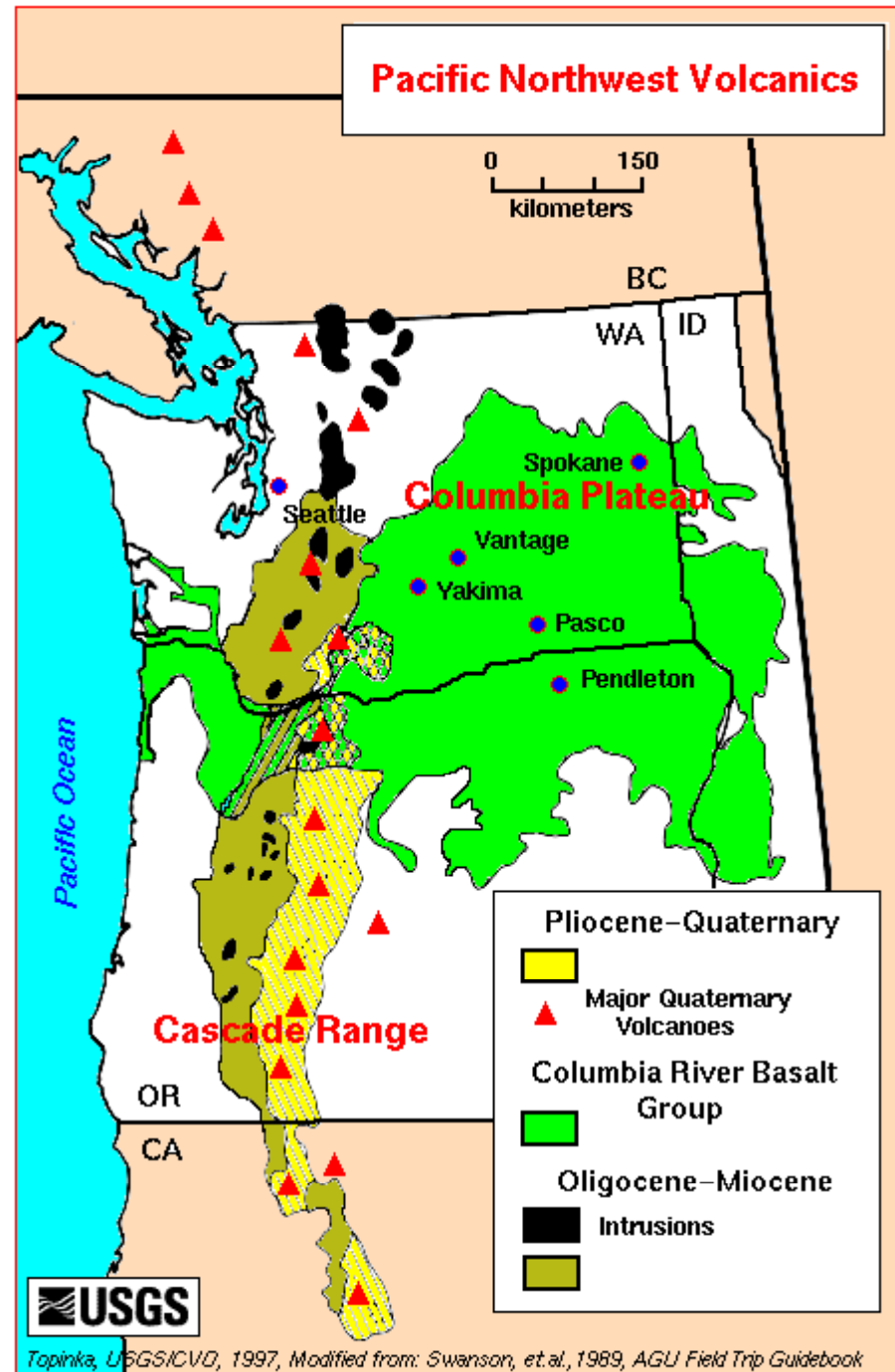
↑ Pressure
Shocked Quartz

↑ Temperature
Microspherules



Flood Basalts

- Millions of cubic kilometers of basalt
- Deposited in ~ 1 million years
- Potential injections of aerosols, water into stratosphere
- Elevation of $p\text{CO}_2$





Flood Basalt, Columbia River Gorge

Timings of Flood Basalt Episodes versus Mass Extinctions and Ocean Anoxia Events

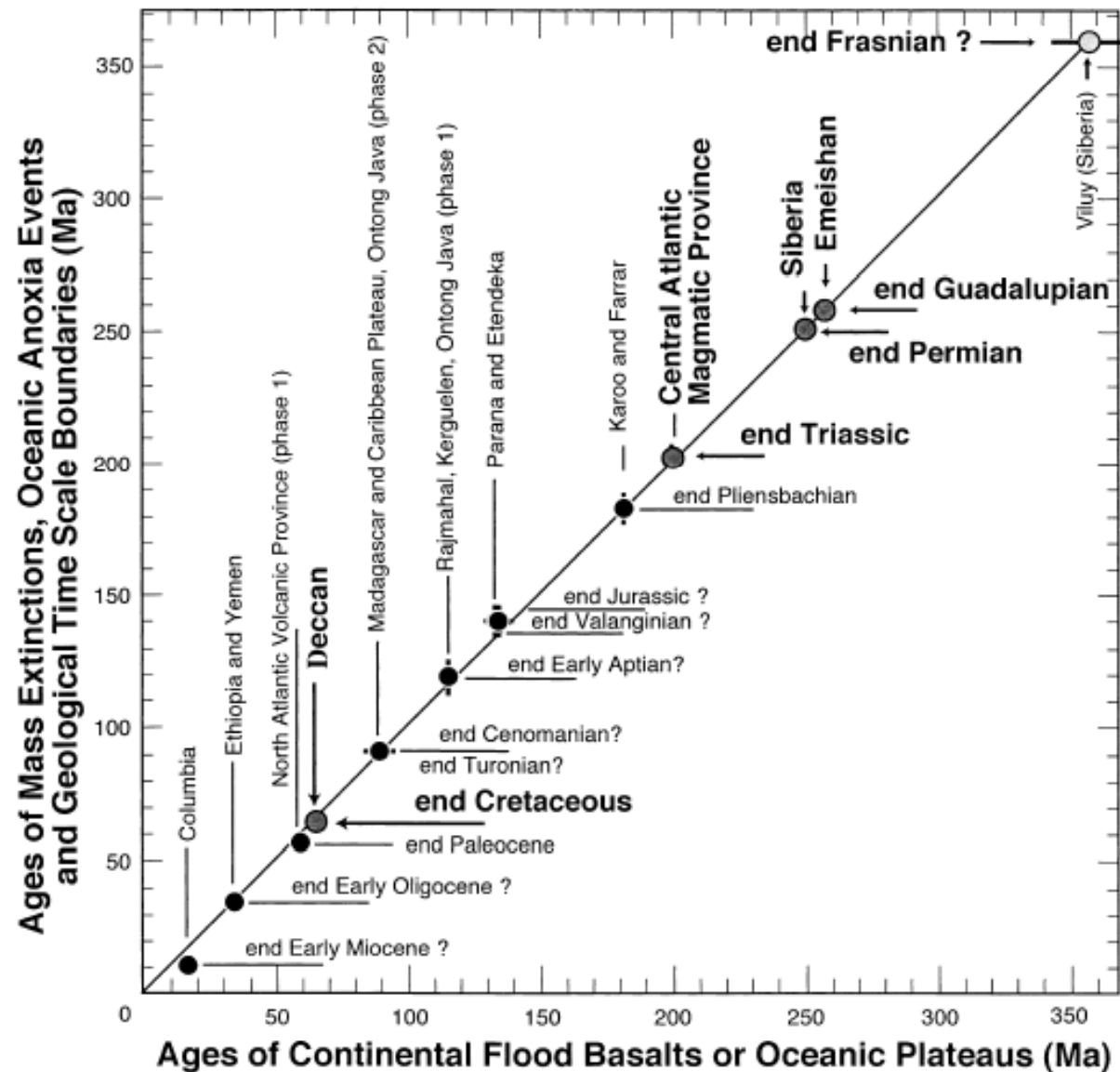
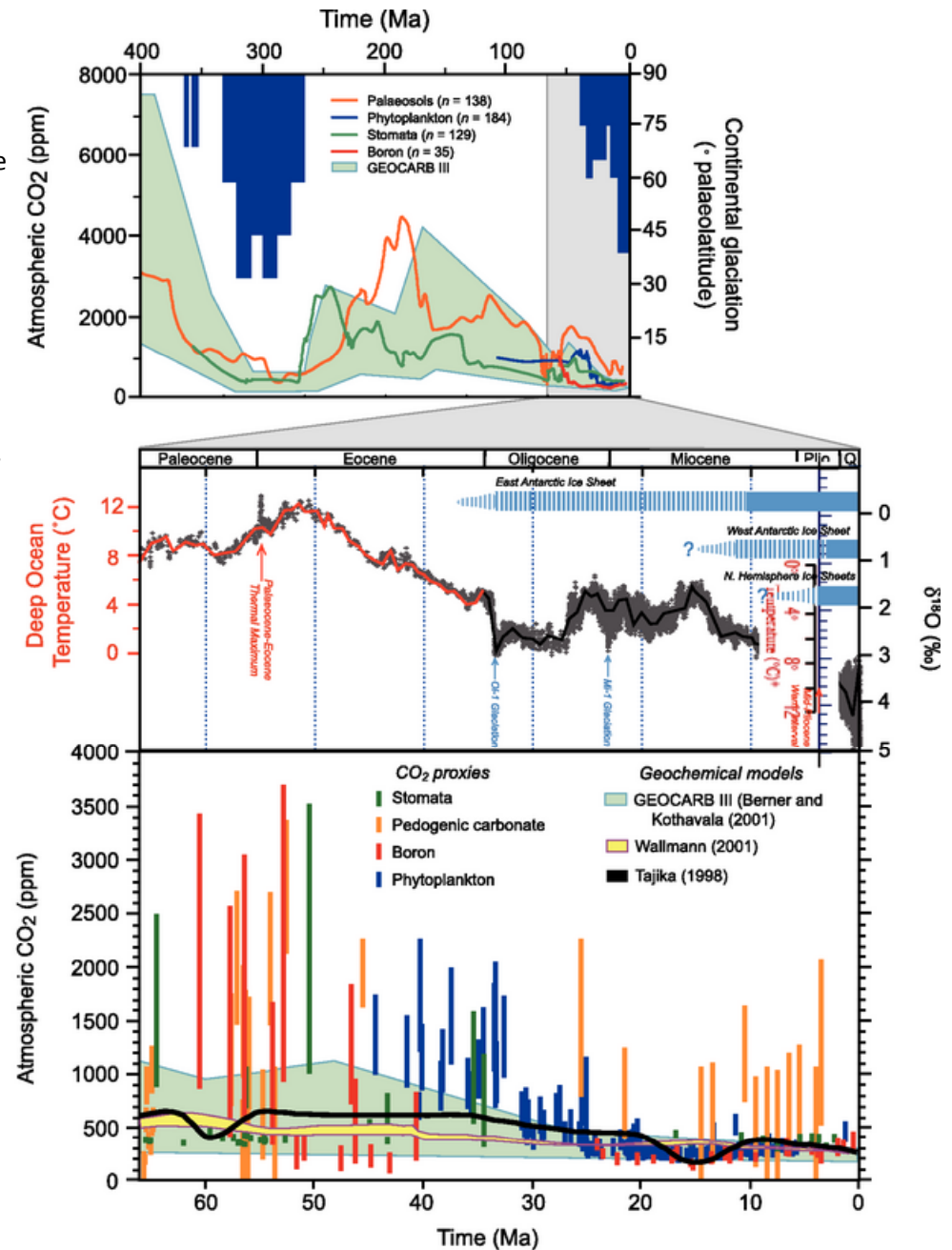


Fig. 1. Correlation between the ages of LIPs (CFBs and OPs) on one hand, and those of mass extinctions and oceanic anoxia events on the other hand (all in Ma). This figure is updated from [31] and some later versions; see also [143] for what may be the first such plot. Values are from Table 1 and are discussed in the text. Uncertainties are visible only when they are larger than the diameters of the dots corresponding to individual events. The four largest recent mass extinctions and corresponding traps are in dark grey, the previous one in light grey is being radiometrically dated.

Courtillot and Rennes,
*Comptes Rendus
Geosciences*, 2003

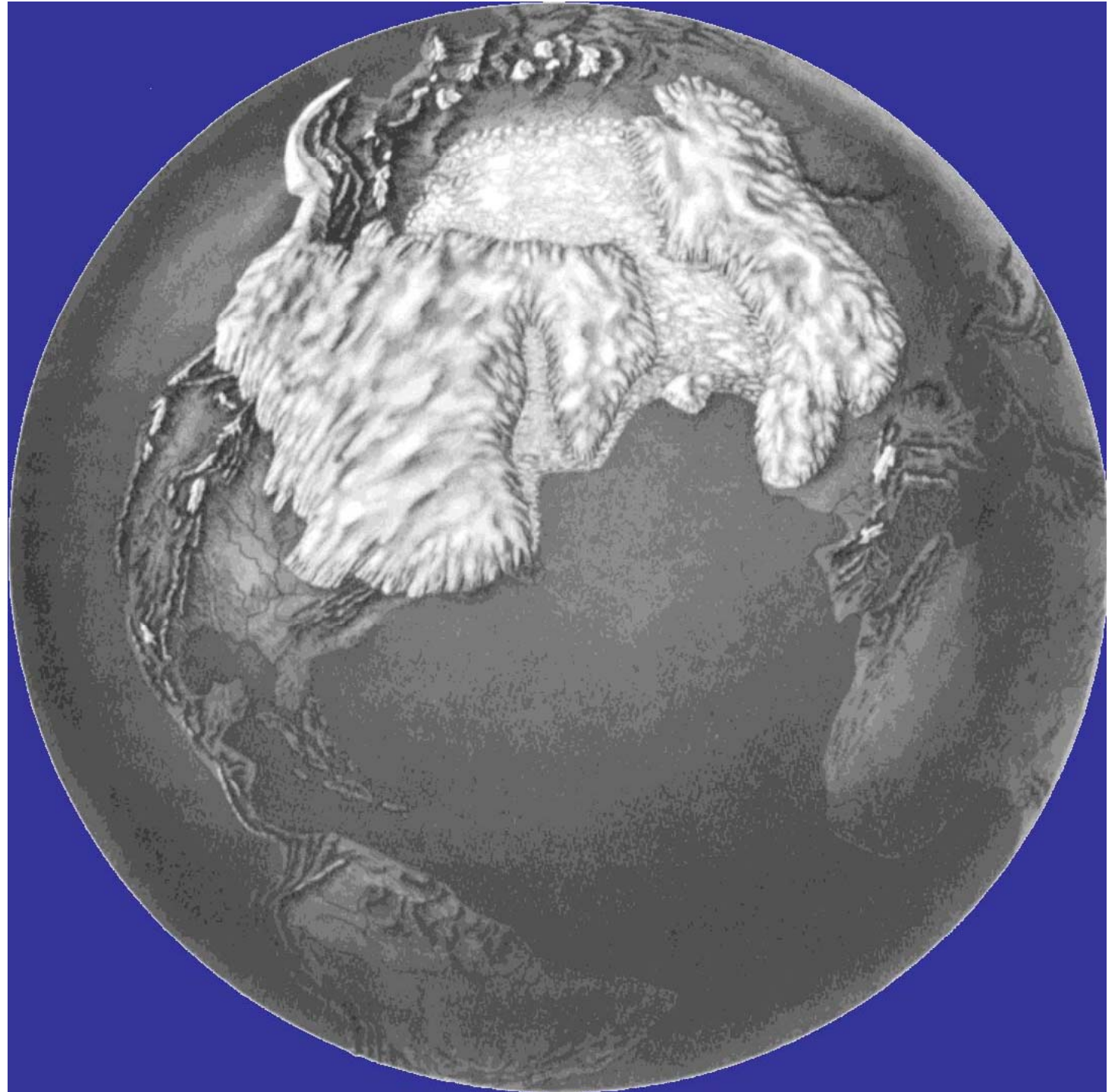
CO₂ and Climate

Figure 6.1. (Top) Atmospheric CO₂ and continental glaciation 400 Ma to present. Vertical blue bars mark the timing and palaeolatitudinal extent of ice sheets (after Crowley, 1998). Plotted CO₂ records represent five-point running averages from each of the four major proxies (see Royer, 2006 for details of compilation). Also plotted are the plausible ranges of CO₂ from the geochemical carbon cycle model GEOCARB III (Berner and Kothavala, 2001). All data have been adjusted to the Gradstein et al. (2004) time scale. (Middle) Global compilation of deep-sea benthic foraminifera ¹⁸O isotope records from 40 Deep Sea Drilling Program and Ocean Drilling Program sites (Zachos et al., 2001) updated with high-resolution records for the Eocene through Miocene interval (Billups et al., 2002; Bohaty and Zachos, 2003; Lear et al., 2004). Most data were derived from analyses of two common and long-lived benthic taxa, Cibicidoides and Nuttallides. To correct for genus-specific isotope vital effects, the ¹⁸O values were adjusted by +0.64 and +0.4 (Shackleton et al., 1984), respectively. The ages are relative to the geomagnetic polarity time scale of Berggren et al. (1995). The raw data were smoothed using a five-point running mean, and curve-fitted with a locally weighted mean. The ¹⁸O temperature values assume an ice-free ocean (−1.0‰ Standard Mean Ocean Water), and thus only apply to the time preceding large-scale antarctic glaciation (~35 Ma). After the early Oligocene much of the variability (~70%) in the ¹⁸O record reflects changes in antarctic and Northern Hemisphere ice volume, which is represented by light blue horizontal bars (e.g., Hambrey et al., 1991; Wise et al., 1991; Ehrmann and Mackensen, 1992). Where the bars are dashed, they represent periods of ephemeral ice or ice sheets smaller than present, while the solid bars represent ice sheets of modern or greater size. The evolution and stability of the West Antarctic Ice Sheet (e.g., Lemasurier and Rocchi, 2005) remains an important area of uncertainty that could affect estimates of future sea level rise. (Bottom) Detailed record of CO₂ for the last 65 Myr. Individual records of CO₂ and associated errors are colour-coded by proxy method; when possible, records are based on replicate samples (see Royer, 2006 for details and data references). Dating errors are typically less than ±1 Myr. The range of error for each CO₂ proxy varies considerably, with estimates based on soil nodules yielding the greatest uncertainty. Also plotted are the plausible ranges of CO₂ from three geochemical carbon cycle models.

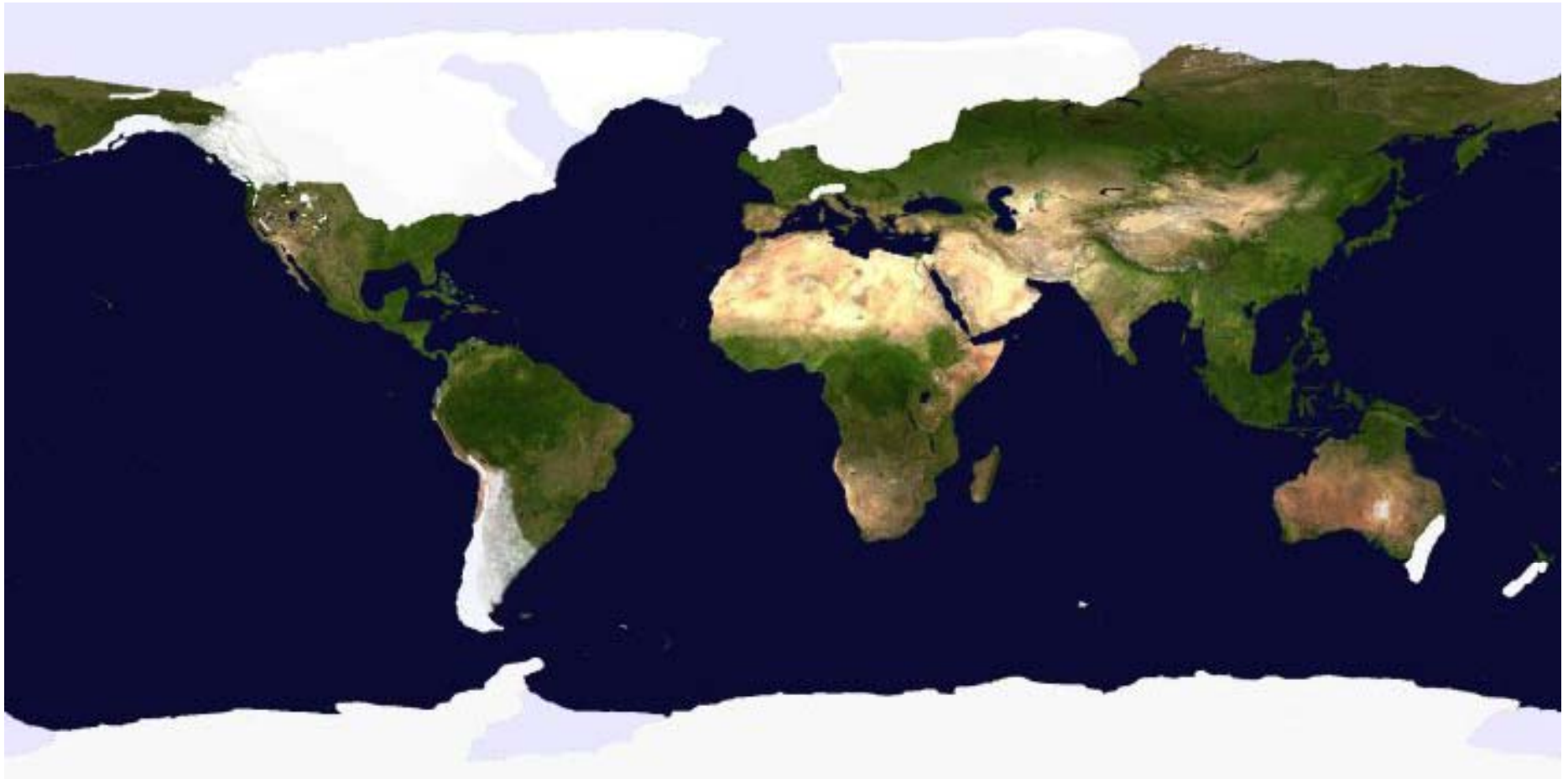


Pleistocene Ice Age Cycles 0-2.65 ma

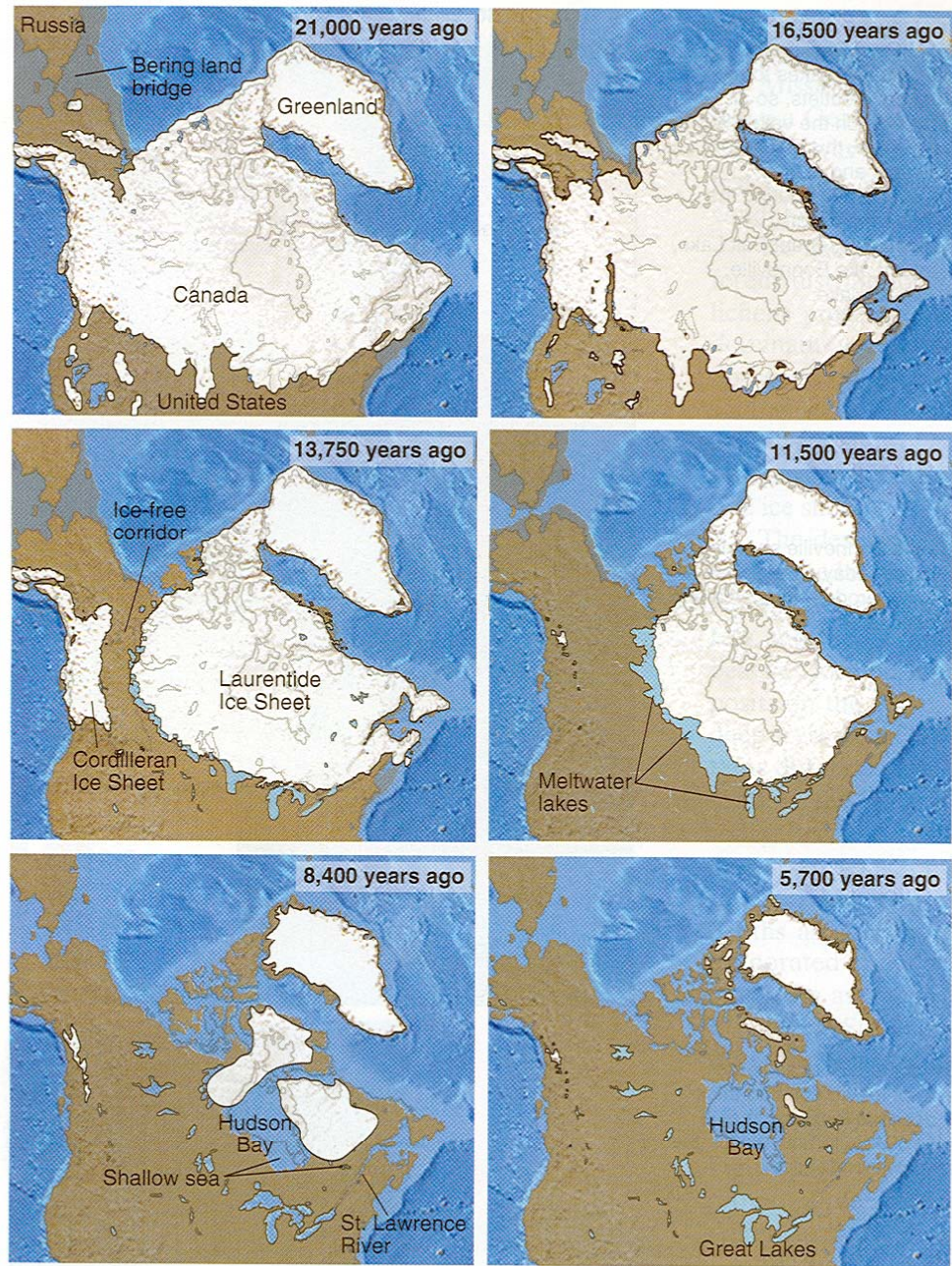
The Last Glacial
Maximum



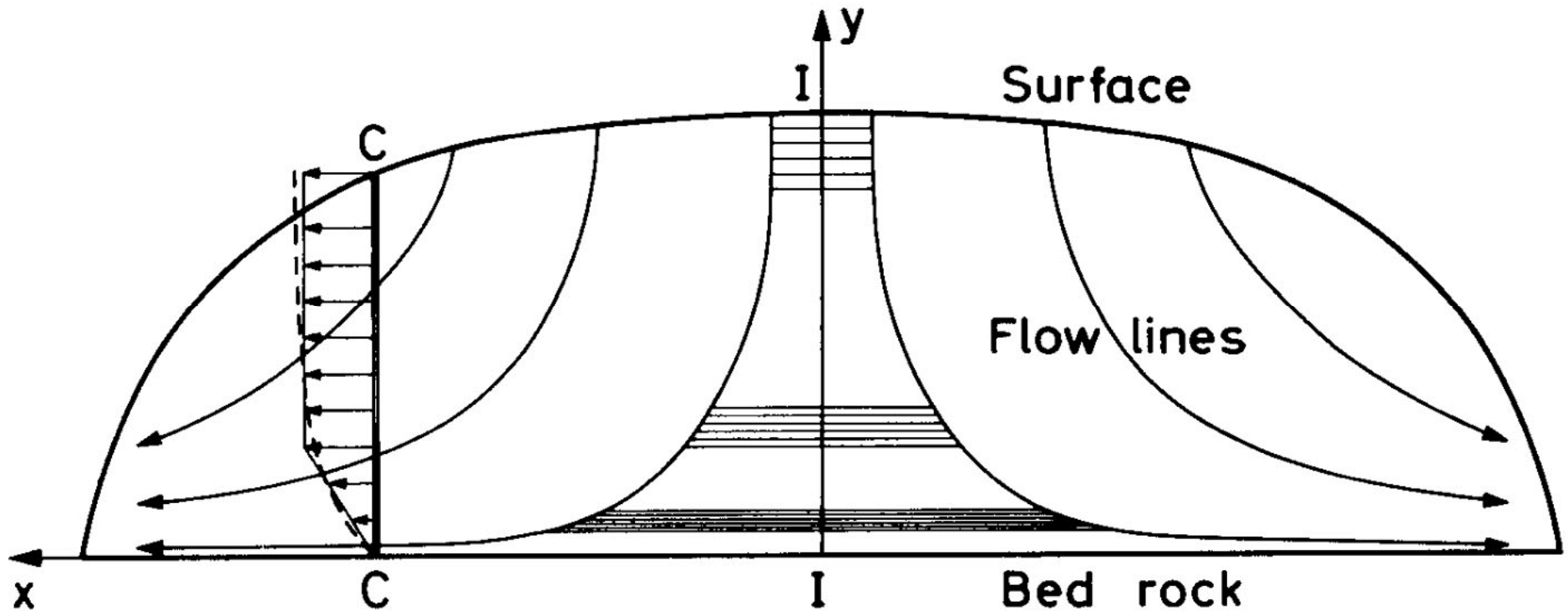
Ice Cover, Last Glacial Maximum (~18,000 years ago)



Rapid pace of deglaciation remains enigmatic



Because they flow, glaciers are filled from their summits:

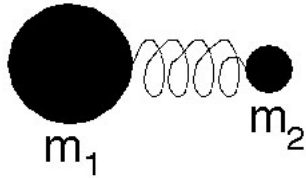


Vertical cross section of an ice sheet resting on a horizontal subsurface. Ice particles deposited on the snow surface will follow lines that travel closer to the base the farther inland the site of deposition. An ice mass formed around the divide (I-I) will be plastically deformed (thinned) with depth as suggested by the lined areas. The dashed curve along the vertical ice core (C-C) shows the calculated horizontal velocity profile V_x (Weertman 1968b). The horizontal arrows along C-C show the adopted approximation to V_x (Dansgaard et al. 1969).

Two geochemical tools:

1. Stable isotope ratios:

$$\delta^{18}\text{O} = \left[\frac{(^{18}\text{O}/^{16}\text{O})_{\text{sample}}}{(^{18}\text{O}/^{16}\text{O})_{\text{standard}}} - 1 \right] \times 1000$$

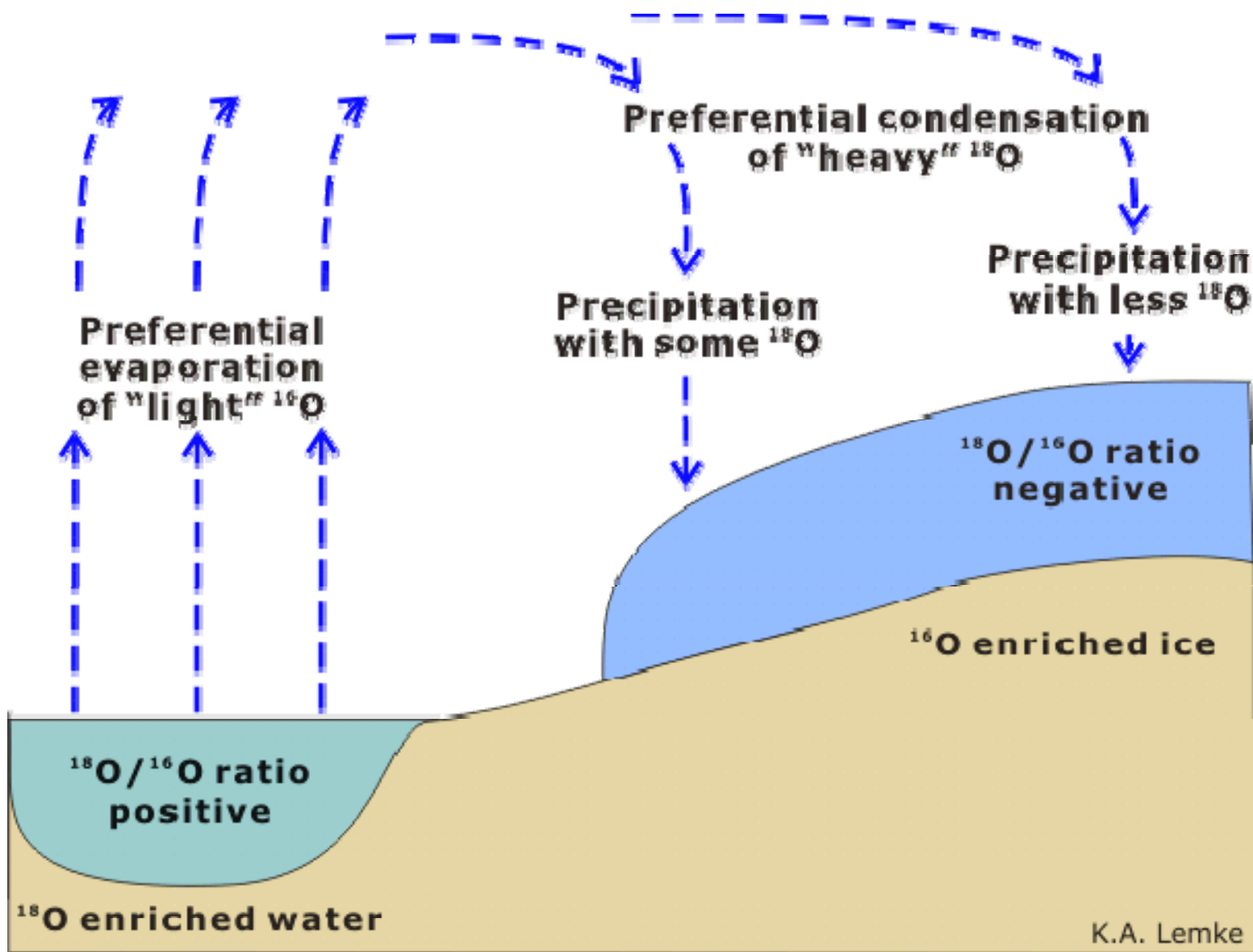


mass-dependent isotope fractionation

2. Triple stable isotope ratios:

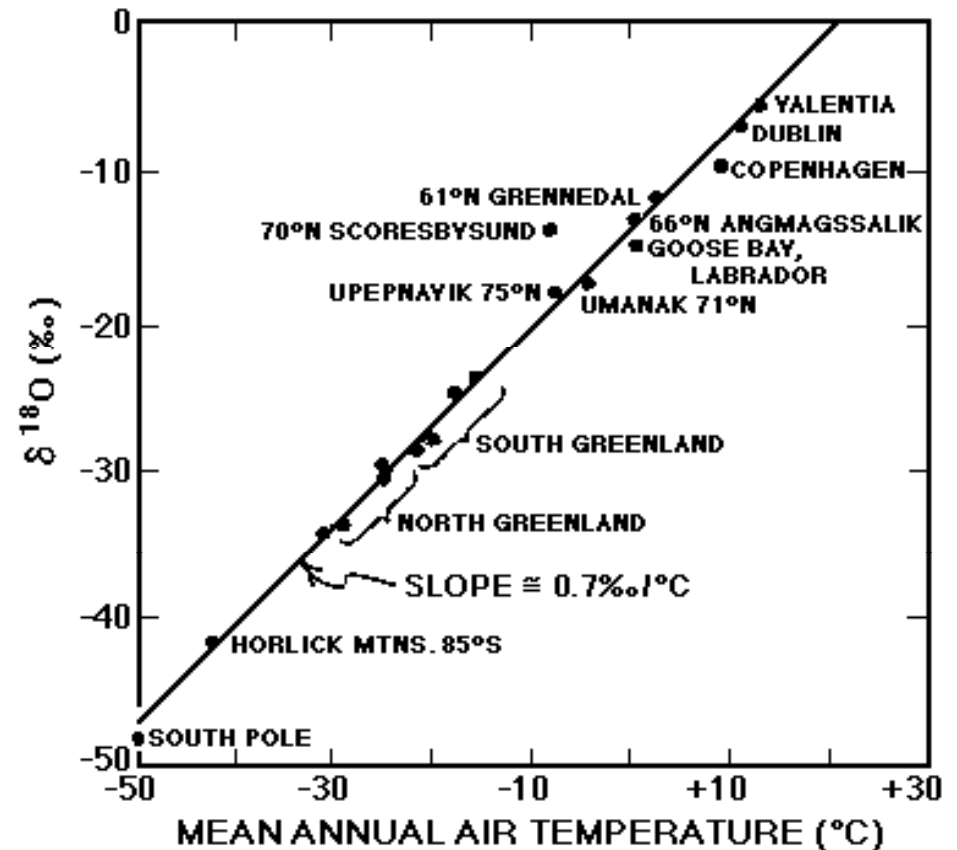
$$\Delta^{33}\text{S} = \delta^{33}\text{S} - 0.515 \delta^{34}\text{S}$$

mass-independent isotope fractionation



K.A. Lemke

Strong correlation between the isotopic composition of snow and mean annual air temperature in the present climate



Observed $\delta^{18}\text{O}$ in average annual precipitation as a function of mean annual air temperature (Dansgaard, 1964). Note that all the points on this graph are for high latitudes ($>45^\circ$). The $\delta^{18}\text{O}$ values are calculated as follows:

$$\delta^{18}\text{O} = \frac{^{18}\text{O}/^{16}\text{O} \text{ sample} - ^{18}\text{O}/^{16}\text{O} \text{ std.}}{^{18}\text{O}/^{16}\text{O} \text{ std.}} \times 1000$$

Broecker, W.S. The Glacial World According to Wally, Copyright © 1993 by Eldigio Press. Reproduced by permission.

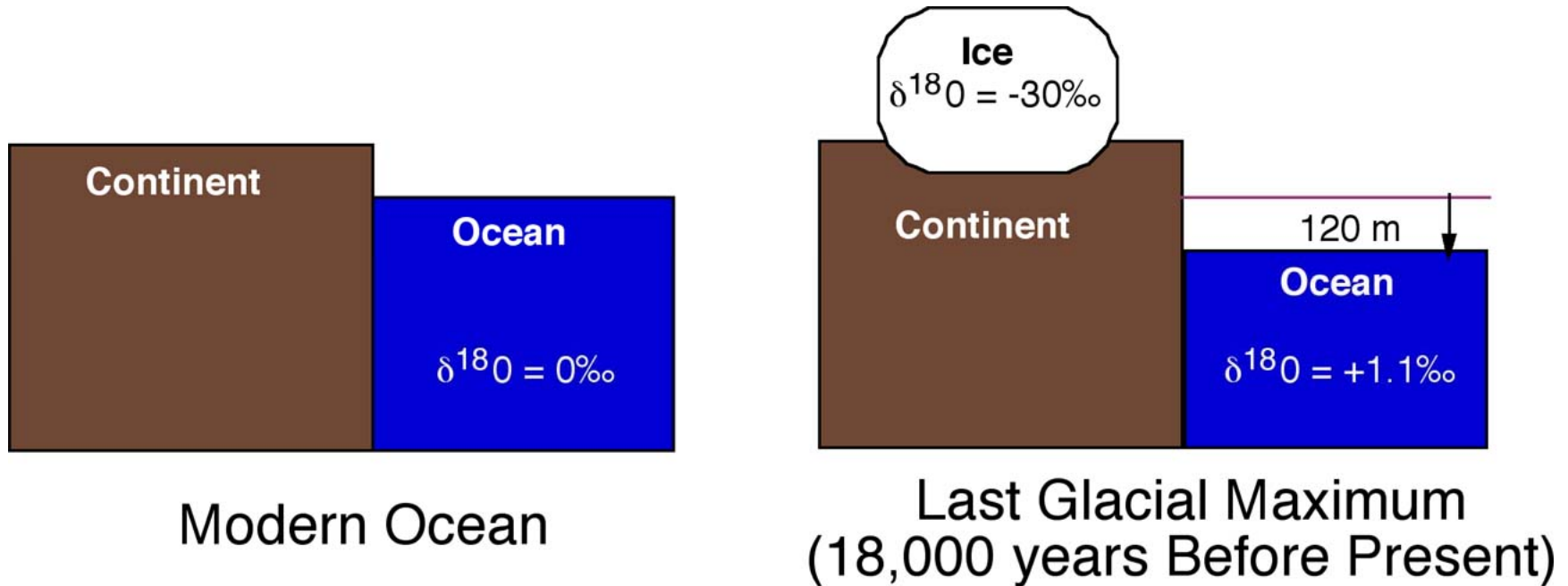




How do we estimate a time scale for a marine sediment core or ice core?

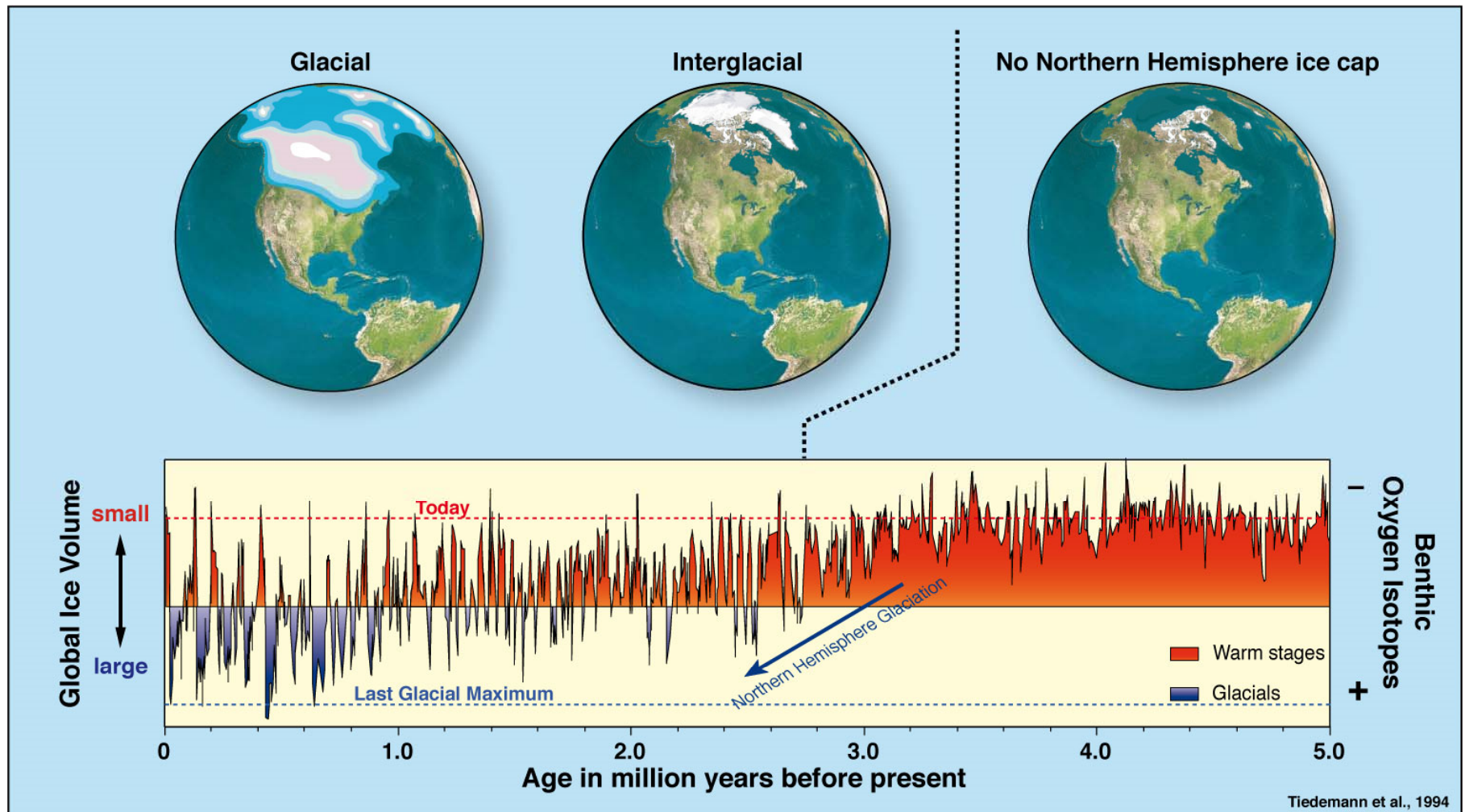
- We measure depth and assume it is an increasing function of the age of the deposit (stratigraphy).
- For sediments <25 kyr BP containing appropriate carbonate or organic) fossils, we can measure the ^{14}C content and determine the age from the atmospheric radiocarbon calibration.
- We can determine the $\delta^{18}\text{O}$ of carbonate fossils and correlate the features to sea level events of known age (from ^{230}Th - ^{234}U dating).
- For sediments with appropriate magnetic minerals, we can measure the magnetic alignment and determine the position of known ($^{40}\text{Ar}/^{39}\text{Ar}$ dated) magnetic reversals.
- In-between these known dates, we must interpolate using some plausible (but un-provable) scheme.

Effect of glaciation on the oxygen isotope composition of the ocean

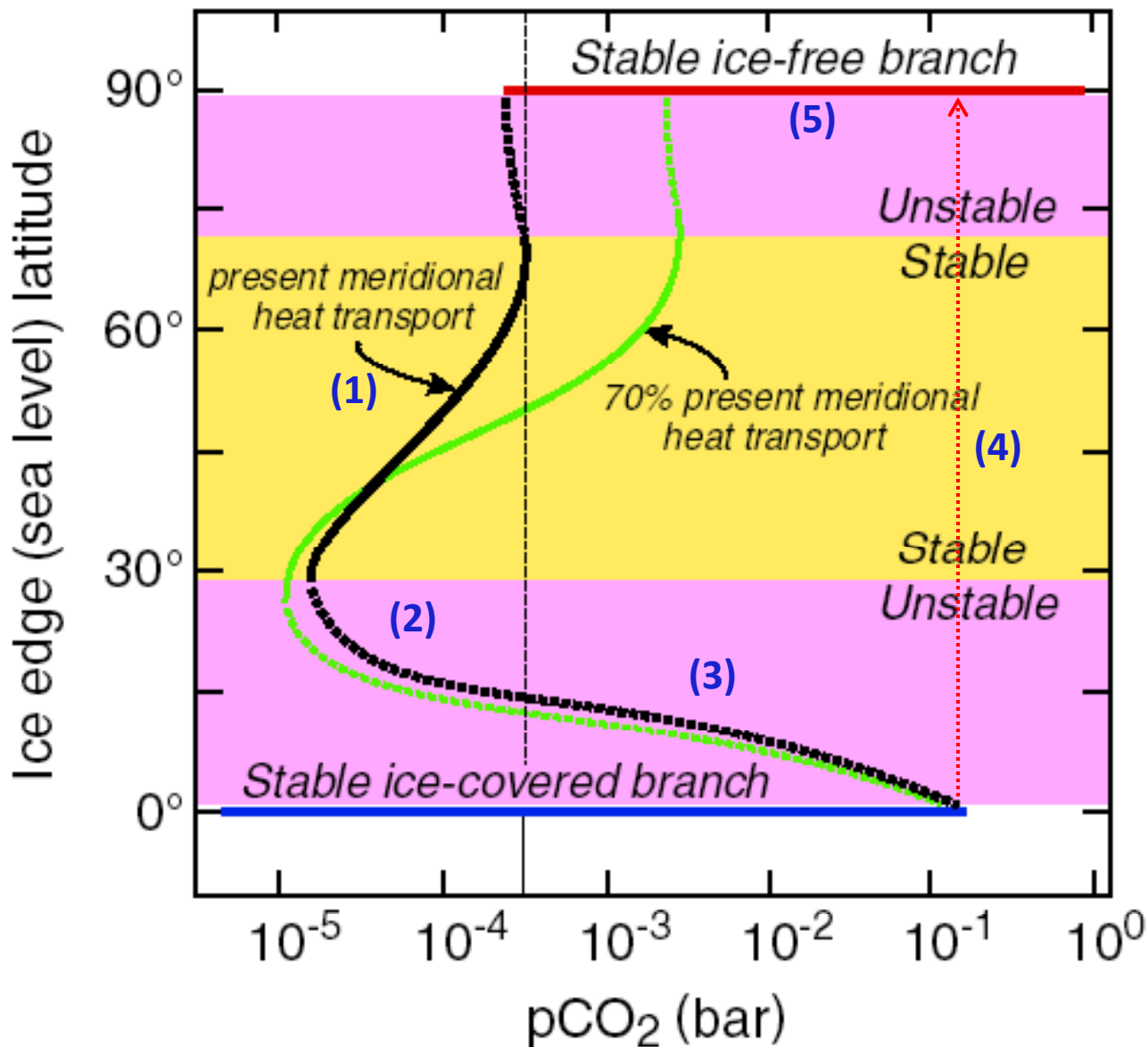


Isotope Mass Balance Equation:

$$M_o \delta_o + M_i \delta_i = M_t \delta_t$$



The benthic oxygen isotope curve reflects the global climate evolution of the last 5 million years, as it is a measure of changes in global ice volume and deep-water temperature. The Pliocene warm period from ~5 to ~3 million years ago is believed to hold clues for assessing future climate change. This time interval, with atmospheric CO₂-concentrations close to modern ones, was significantly warmer than today. High-latitude sea surface temperatures were up to 7°C higher, the modern Northern Hemisphere ice cap over Greenland was absent, and the sea level was about 30 m higher than today. Hence, it represents a possible future climate scenario predicted by numerical models. The long-term increase in oxygen isotope values from ~3–2.5 million years ago marks the development of a permanent Northern Hemisphere ice cap with varying size. The last 3 million years are characterized by alternating glacial and interglacial climate stages, while glacial ice sheets reached their largest size during the last 700,000 years.

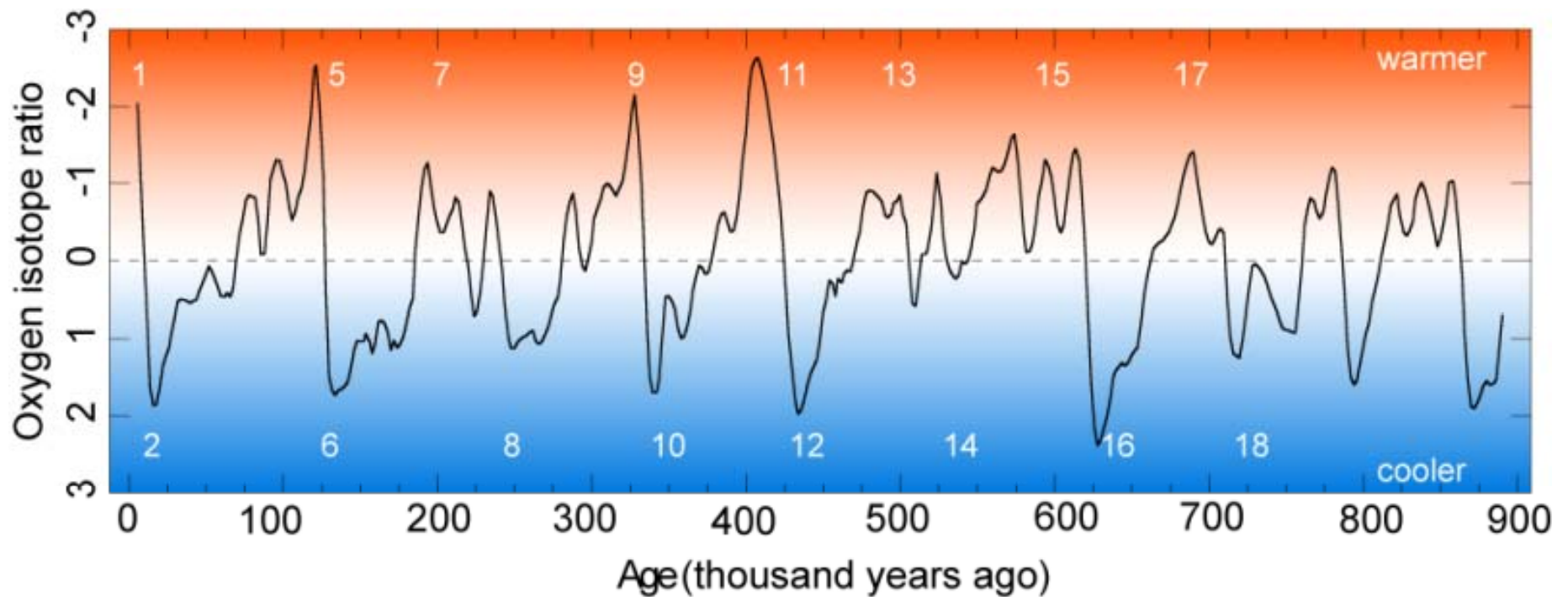


• Runaway Albedo Feedback

1. Eq. continents, incr. weathering, lowers CO₂, slow cooling, equatorward movement of ice.
2. Runaway albedo
3. Weathering shuts down
4. Slow buildup of CO₂ from volcanoes
5. Rapid decay of ice in 10² yr. High T_s from enhanced H₂O-T feedback.
6. Slow CO₂ drawdown from weathering

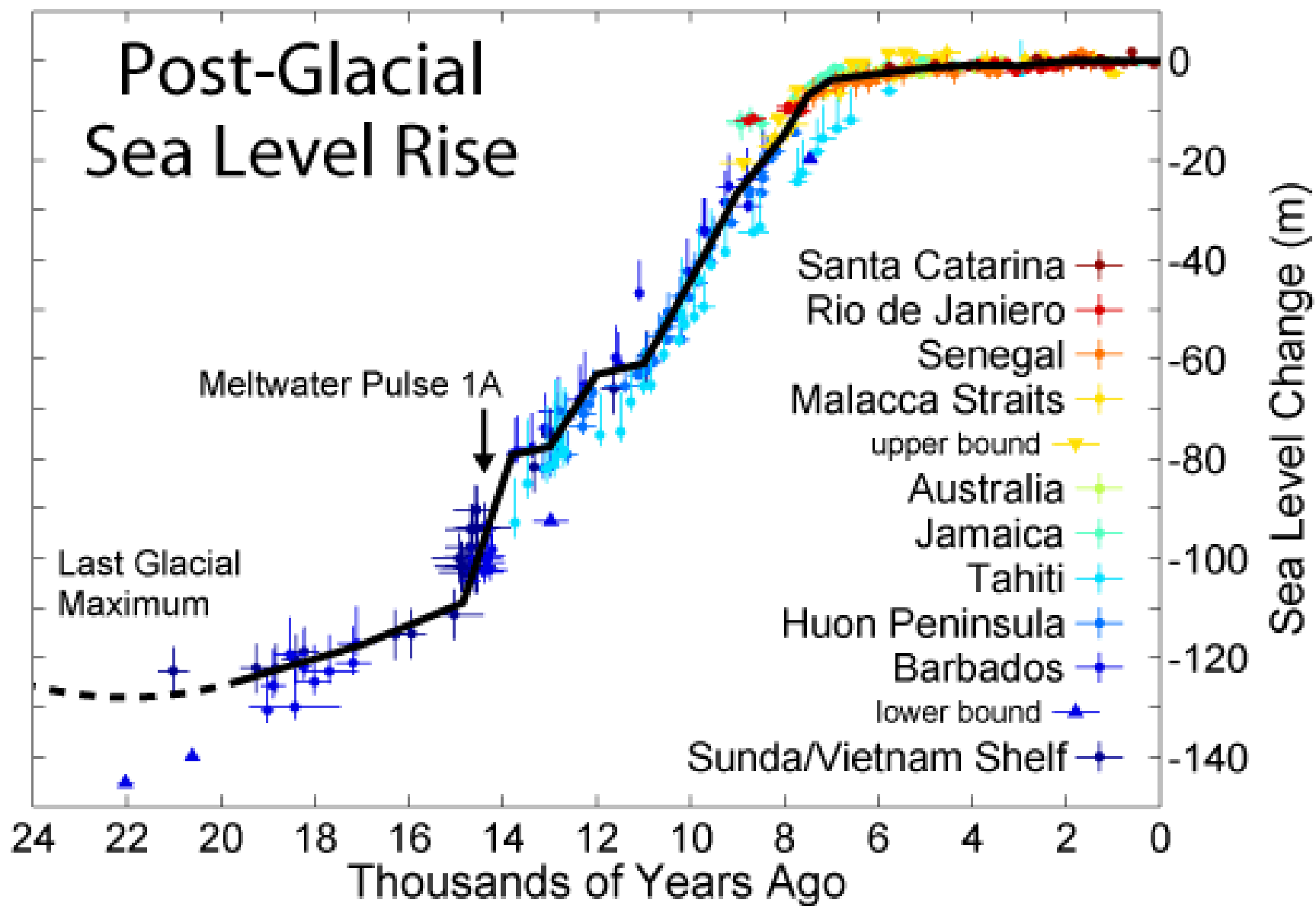
Steady-state ice lines as a function of atmospheric pCO₂, see Caldeira and Kasting (*Nature* **359**: 226, 1992), and Ikeda and Tajika (*Geophys. Res. Lett.* **26**: 349, 1999).

Image from P. Hoffman

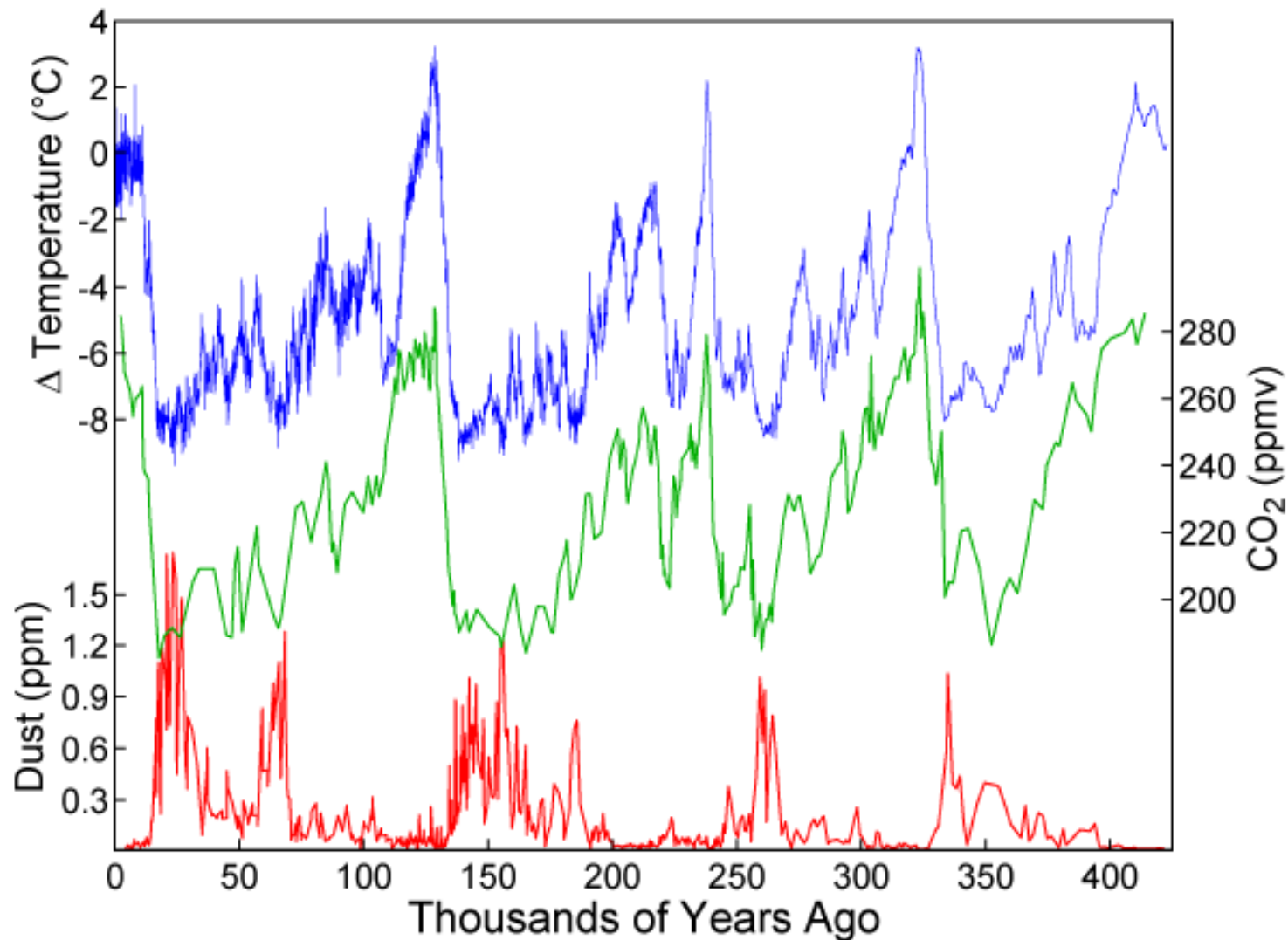


The oxygen isotope ratio ($^{18}\text{O}/^{16}\text{O}$) in oceanic sediment depends on the ancient water temperature and on the extent of the ice volume over continents; it therefore provides a record of past oscillations in the climate and global sea level.

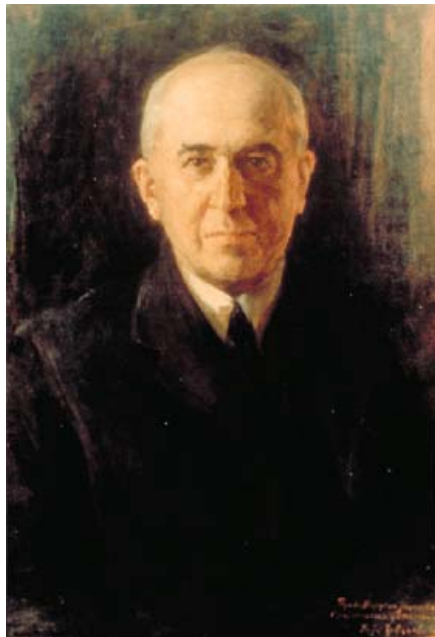
The heavier ^{18}O isotope is relatively less abundant in ice caps and glaciers than in oceanic water. When large ice sheets spread over continents, the sea water and the carbonatic tests of marine organisms became correspondingly richer in ^{18}O . The higher the concentration of ^{18}O in a sediment, the wider the development of continental glaciation at the same geological time. The oxygen isotope stages are progressively numbered from younger to older, with odd numbers referring to warmer periods and even numbers to colder periods. The figure shows the variation of the $^{18}\text{O}/^{16}\text{O}$ ratio during the last 900 kyr and the alternation of glacial – interglacial periods.



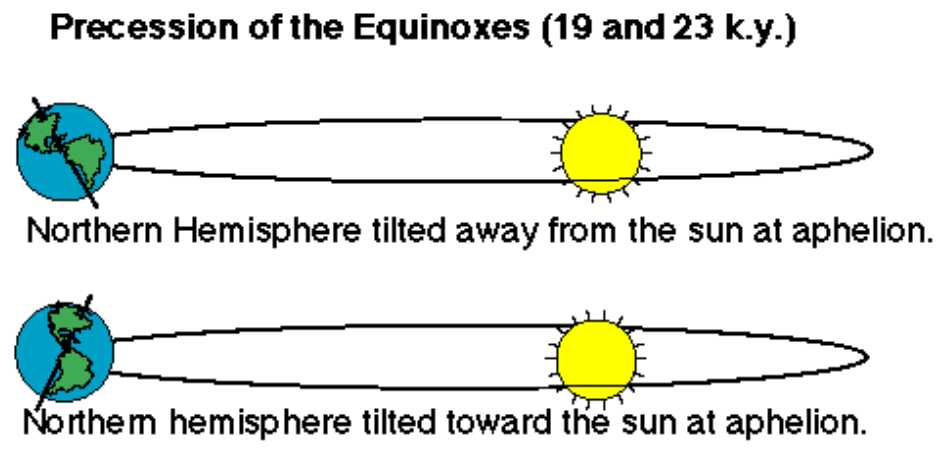
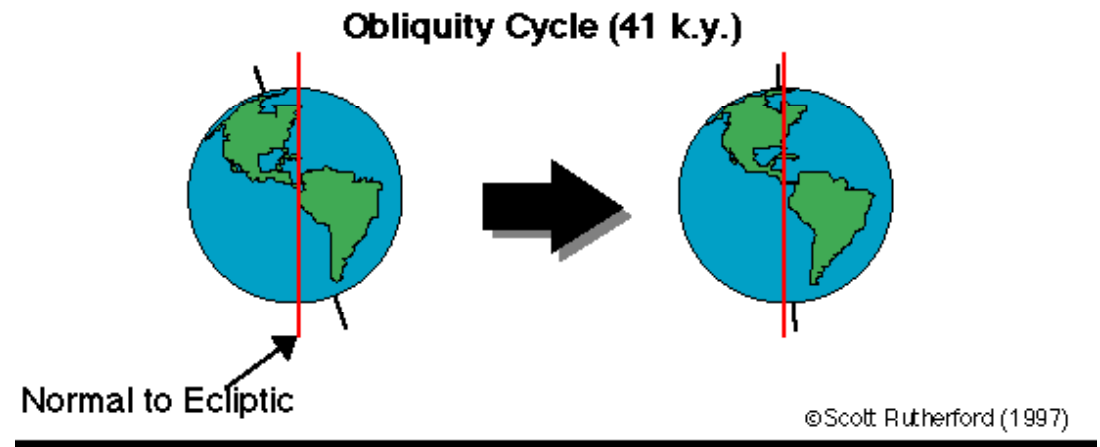
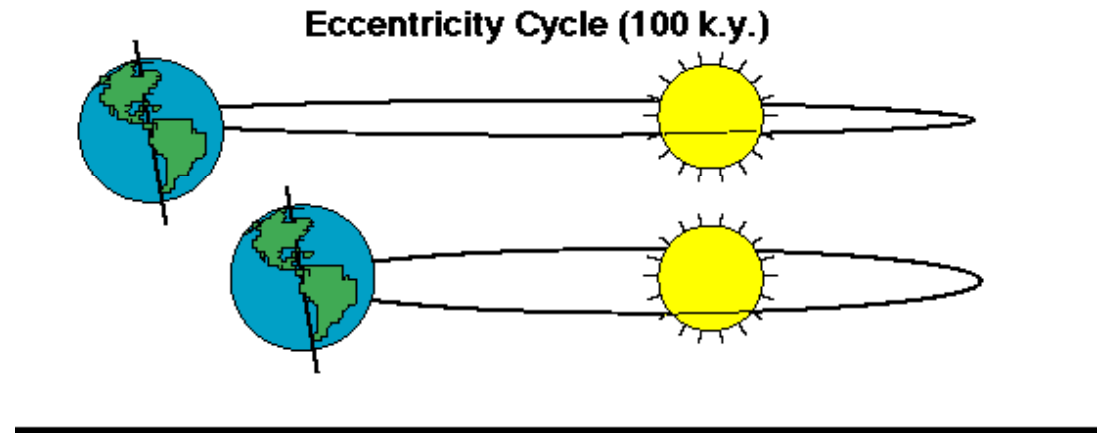
A detailed record of the earth's climate has emerged over the last few decades, from analyses of ice cores and deep sea sediments



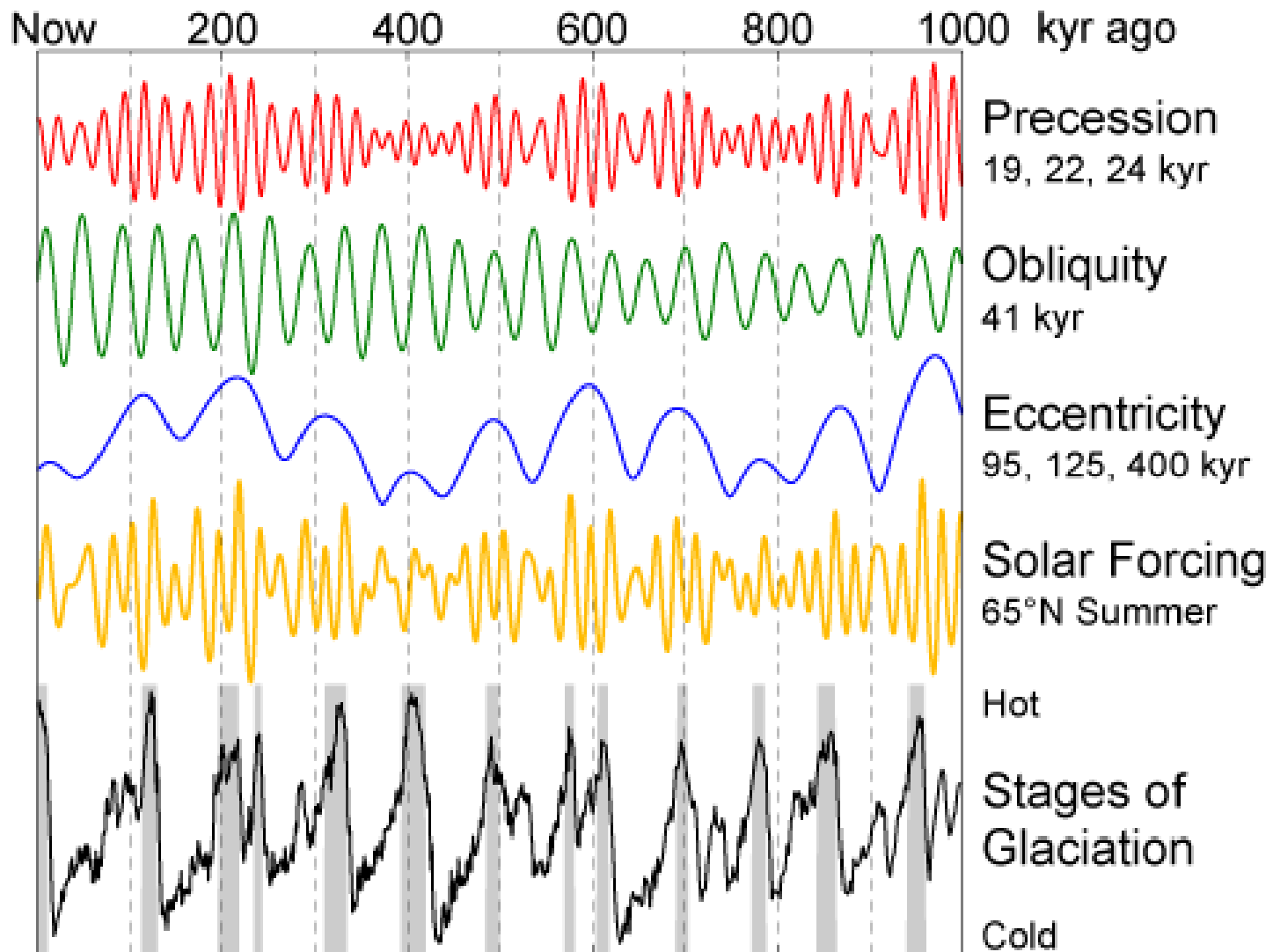
Climate Forcing by Orbital Variations



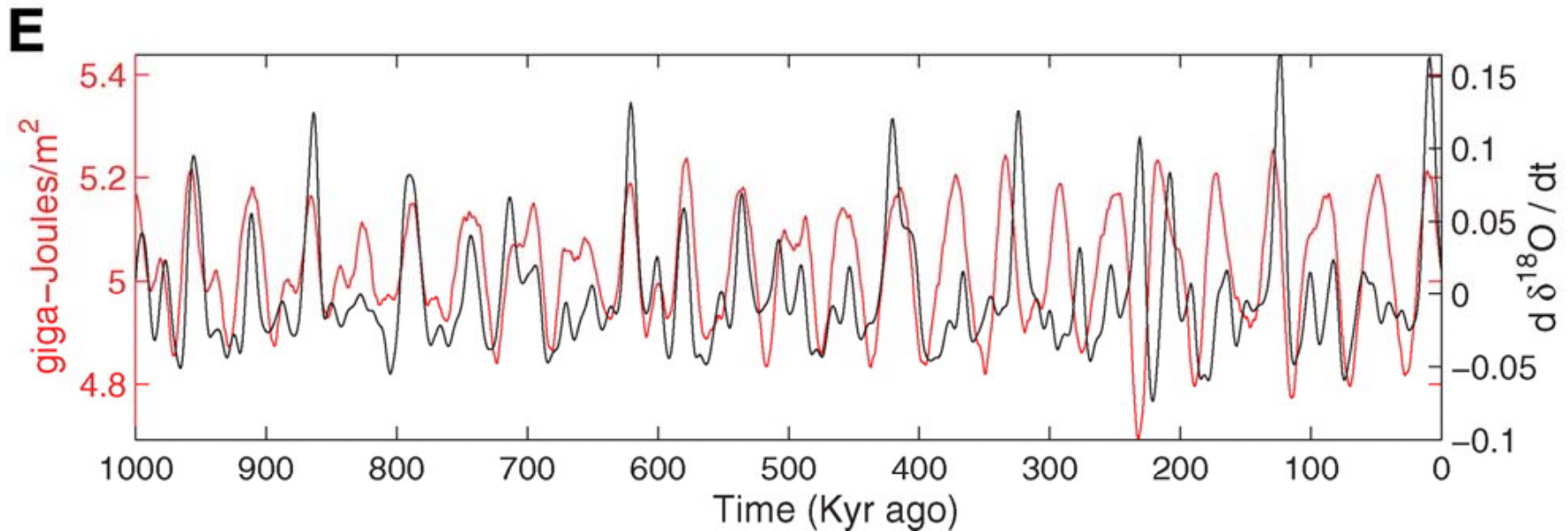
Milutin Milanković, 1879-1958



Climate Forcing and Response



Strong Correlation between High Latitude Summer Insolation and Ice Volume

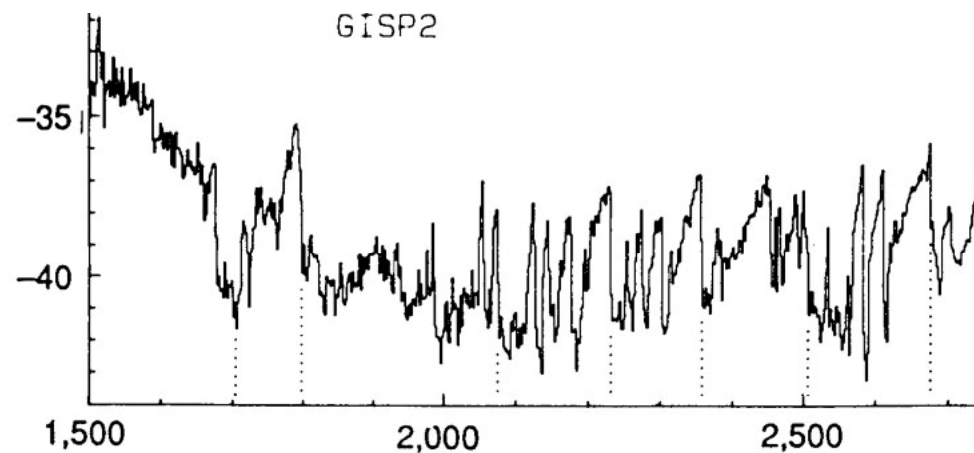


Black: Time rate of change of ice volume

Red: Summer high latitude sunlight

Abrupt climate swings during the past 100,000 years: the Bolling-Allerod, Younger Dryas, and “stadial/interstadial” “Dansgaard-Oeschger cycles

- Between 10,000-65,000 years ago, there were at least 17 abrupt swings between warmer and colder climate events.
- These events were first observed in the Greenland ice cores, but they have now been seen at diverse sites in the Northern Hemisphere including the tropics.
- These events are not observed in the Antarctic ice cores, save possibly in dampened form.



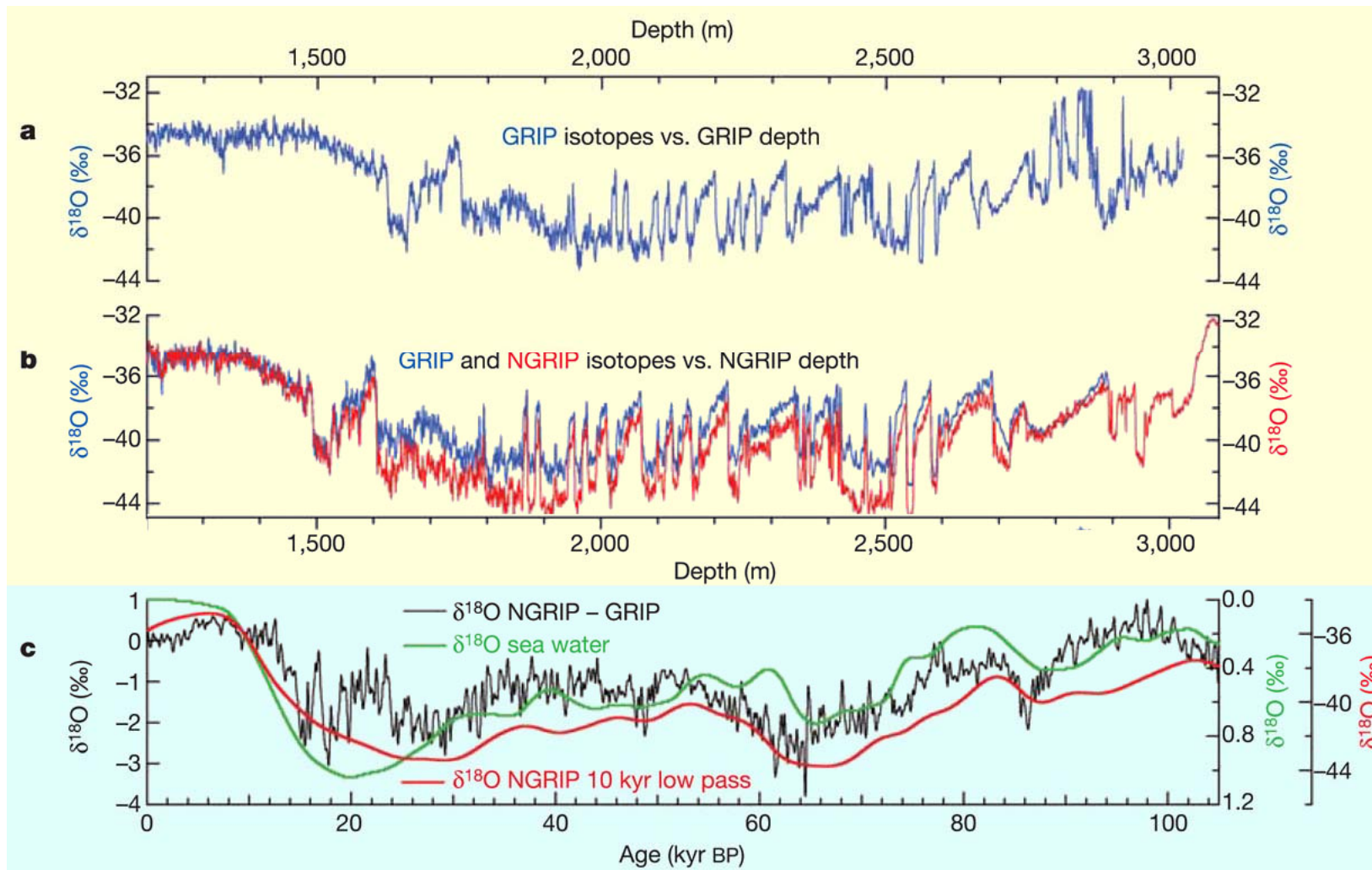
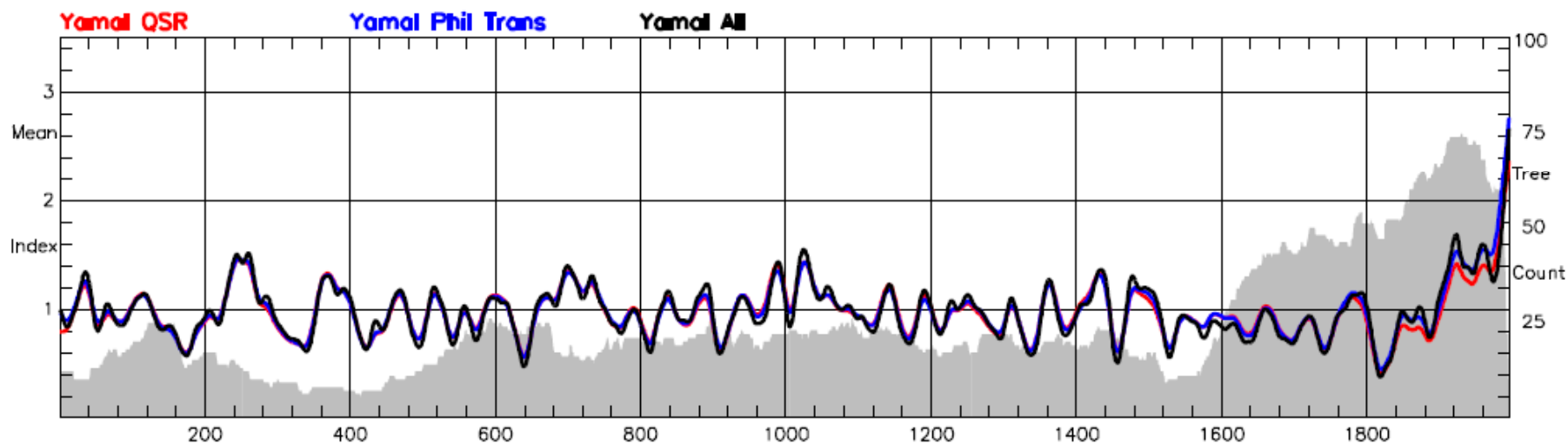


Figure 2 The NGRIP stable oxygen isotopic record compared to the GRIP record. **a**, The GRIP oxygen isotopic profile (blue) with respect to depth at GRIP. Isotopic values ($\delta^{18}\text{O}$) are expressed in ‰ with respect to Vienna Standard Mean Ocean Water (V-SMOW). The measurements have been performed on 55 cm samples with an accuracy of ± 0.1 ‰. **b**, The NGRIP oxygen isotopic profile (red) with respect to depth at NGRIP. For comparison, the GRIP record (blue) has been plotted on the NGRIP depth scale using the rapid transitions as tie points. **c**, The difference between the NGRIP and GRIP oxygen isotopic profiles plotted above on the GRIP2001/ss09sea timescale¹⁵ in 50 yr resolution (black). The record is compared to a record representing sea level changes³⁹ (green) and a 10-kyr smoothed oxygen isotope profile from NGRIP (red).

Dendrochronology

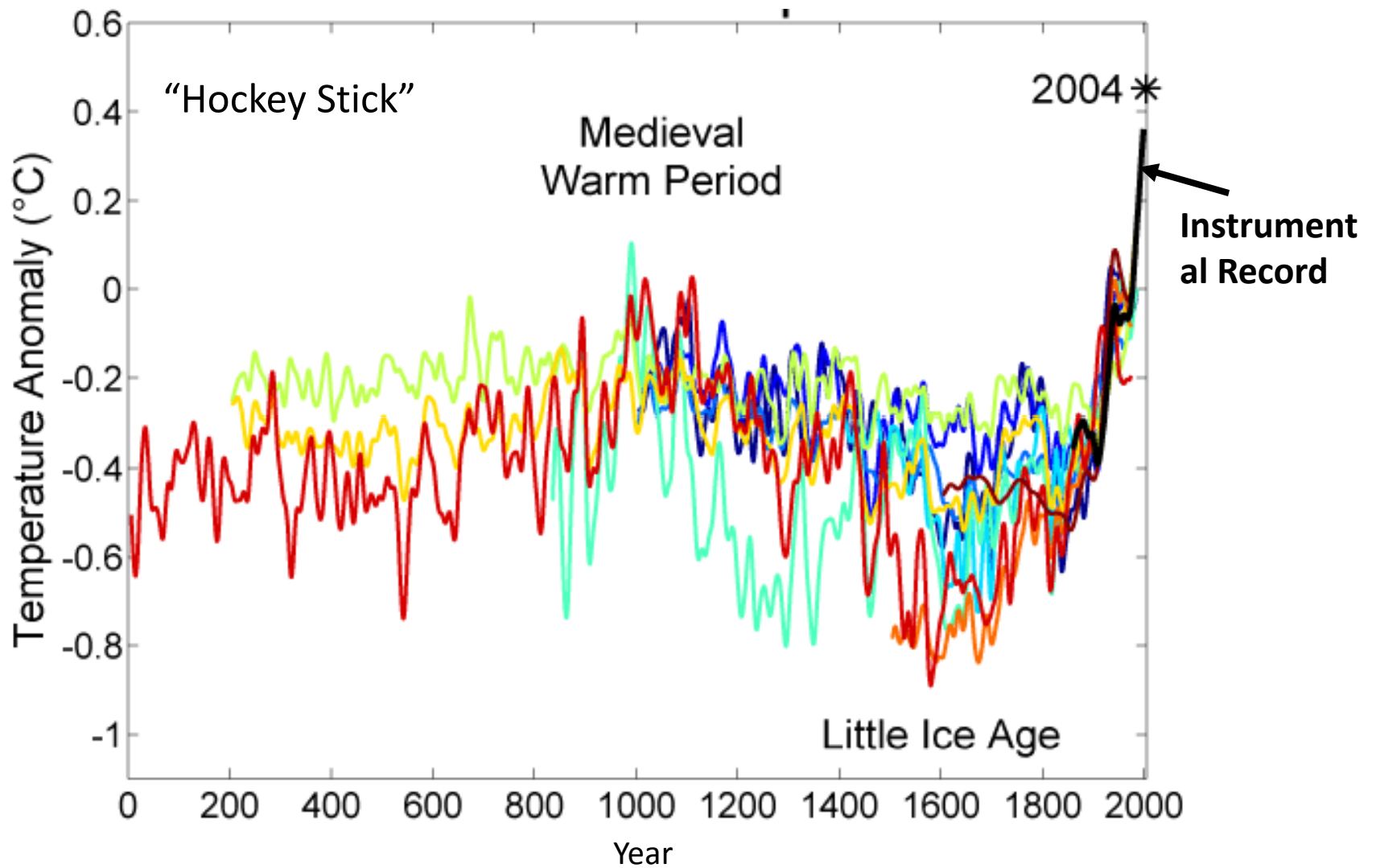


Tree-Ring Proxy for Summer Temperatures in the Yamal Region of Northern Russia



This Figure shows the two earlier versions of the Yamal RCS larch chronology in red (published in Briffa, 2000) and blue (Briffa *et al.*, 2008) compared to the new version, based on all of the currently available data (Yamal_All) for the original (POR, YAD and JAH) sites and including the additional data from the KHAD site (in black). Tree sample counts for this 'new' chronology are shown by the grey shading. The upper panel shows the data smoothed with a 40-year low-pass cubic smoothing spline. The lower panel shows the yearly data from 1800 onwards. All series have been scaled so the yearly data have the same mean and standard deviation as the Yamal_All series over the period 1-1600.

Paleo reconstructions of temperature change over the last 2000 years



Temperature inferences from glacial ice core oxygen isotopes (Thompson, 2003)

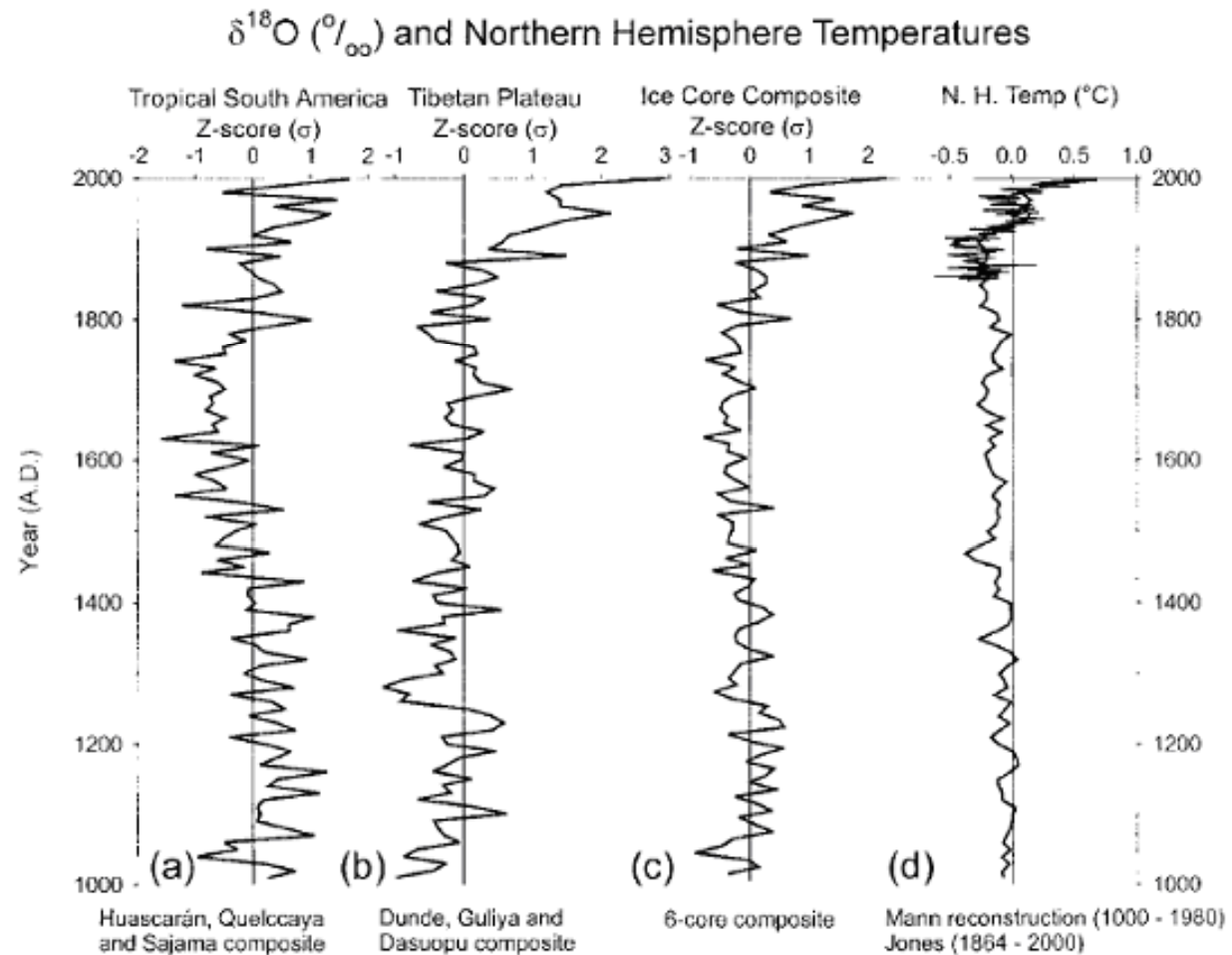
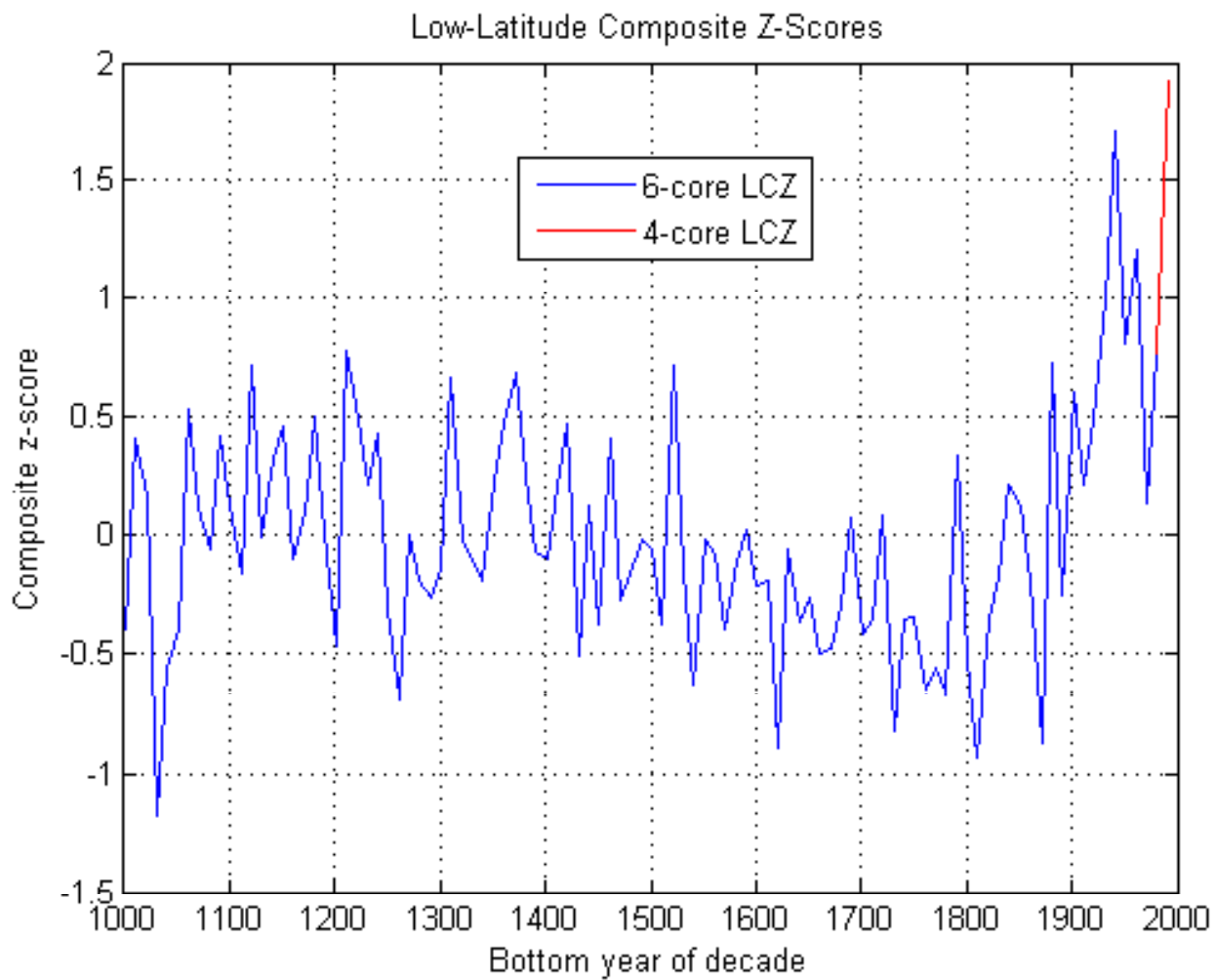


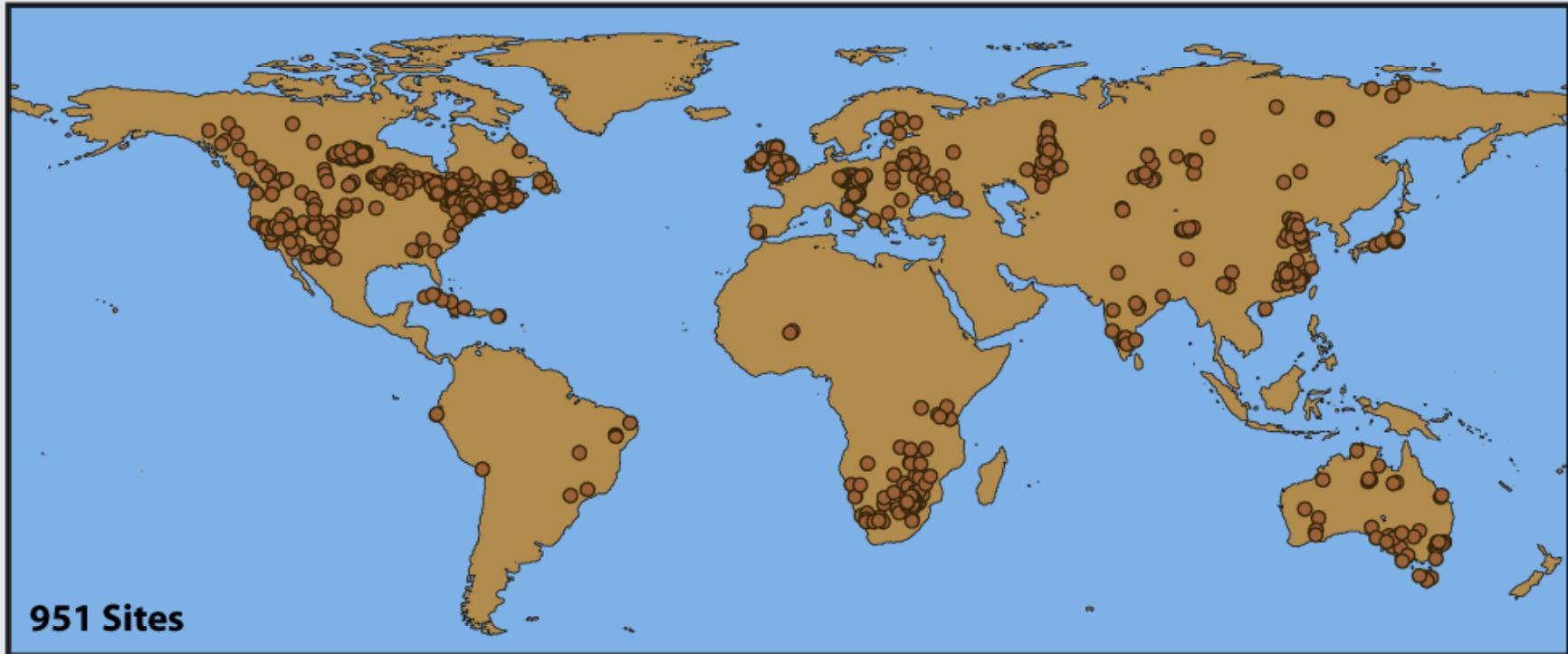
Figure 7. Regional composites, shown as z-scores, for the last millennium were constructed from the decadal averages of $\delta^{18}\text{O}_{\text{ice}}$ from three Andean ice cores (a) and three Tibetan ice cores (b). The composite of all six low latitude cores is shown in (c). The measured (Jones et al., 1999) and reconstructed (Mann et al., 1999) Northern Hemisphere temperatures are shown in (d) and are plotted as deviations (°C) from their respective 1961–1990 means. Note that the decadal average of $\delta^{18}\text{O}_{\text{ice}}$ for 1991 to 2000 is based on the 1991 to 1997 annual values for the Dasuopu core drilled in 1997 and on the 1991–1997 annual values for the Sajama drilled in 1997. The Quelccaya $\delta^{18}\text{O}_{\text{ice}}$ history has been updated to 2000 by drilling new shallow cores.



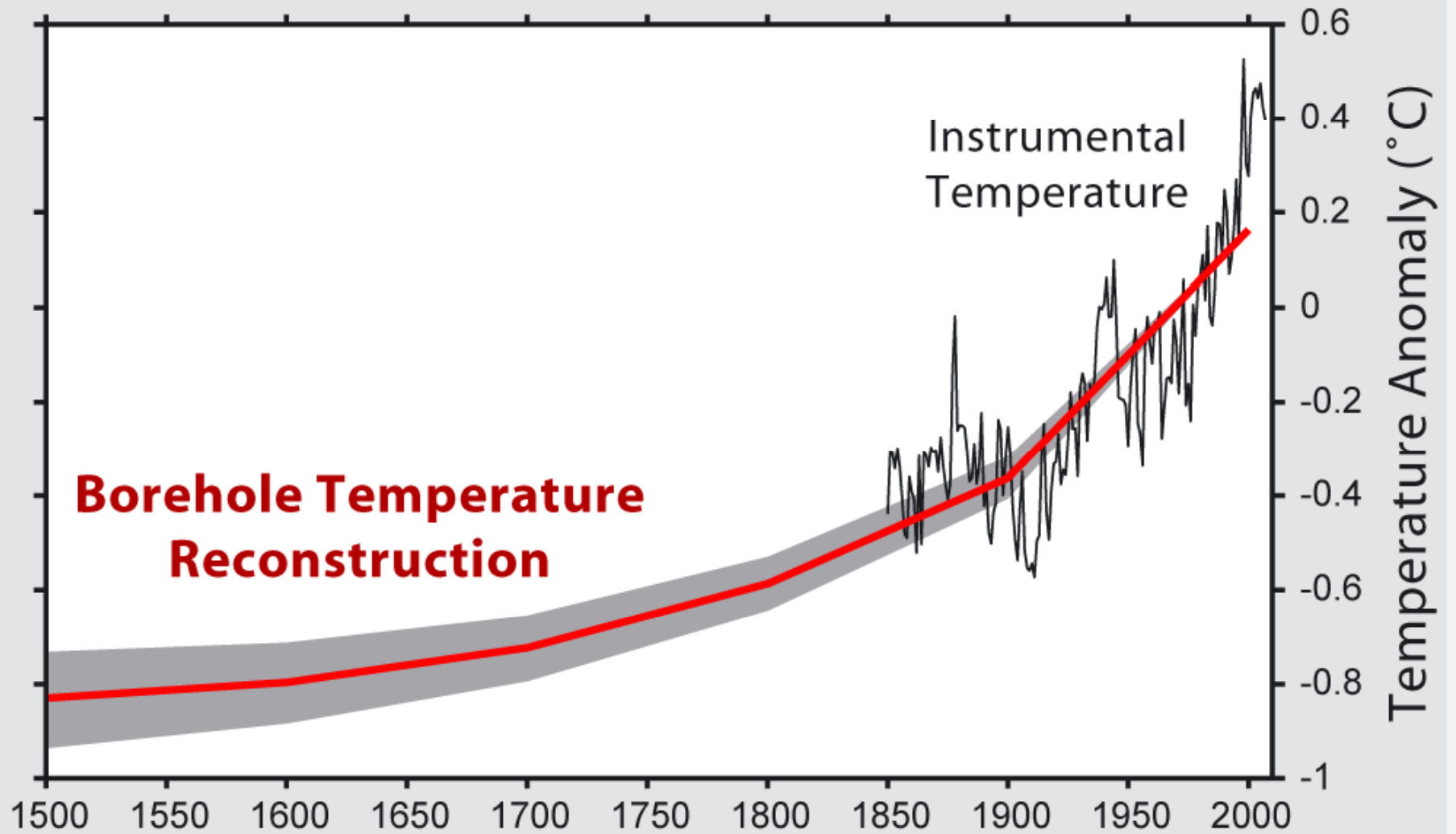
Low-latitude composite of Thompson (2003) data

Borehole Temperatures

Borehole Temperature Measurement Sites

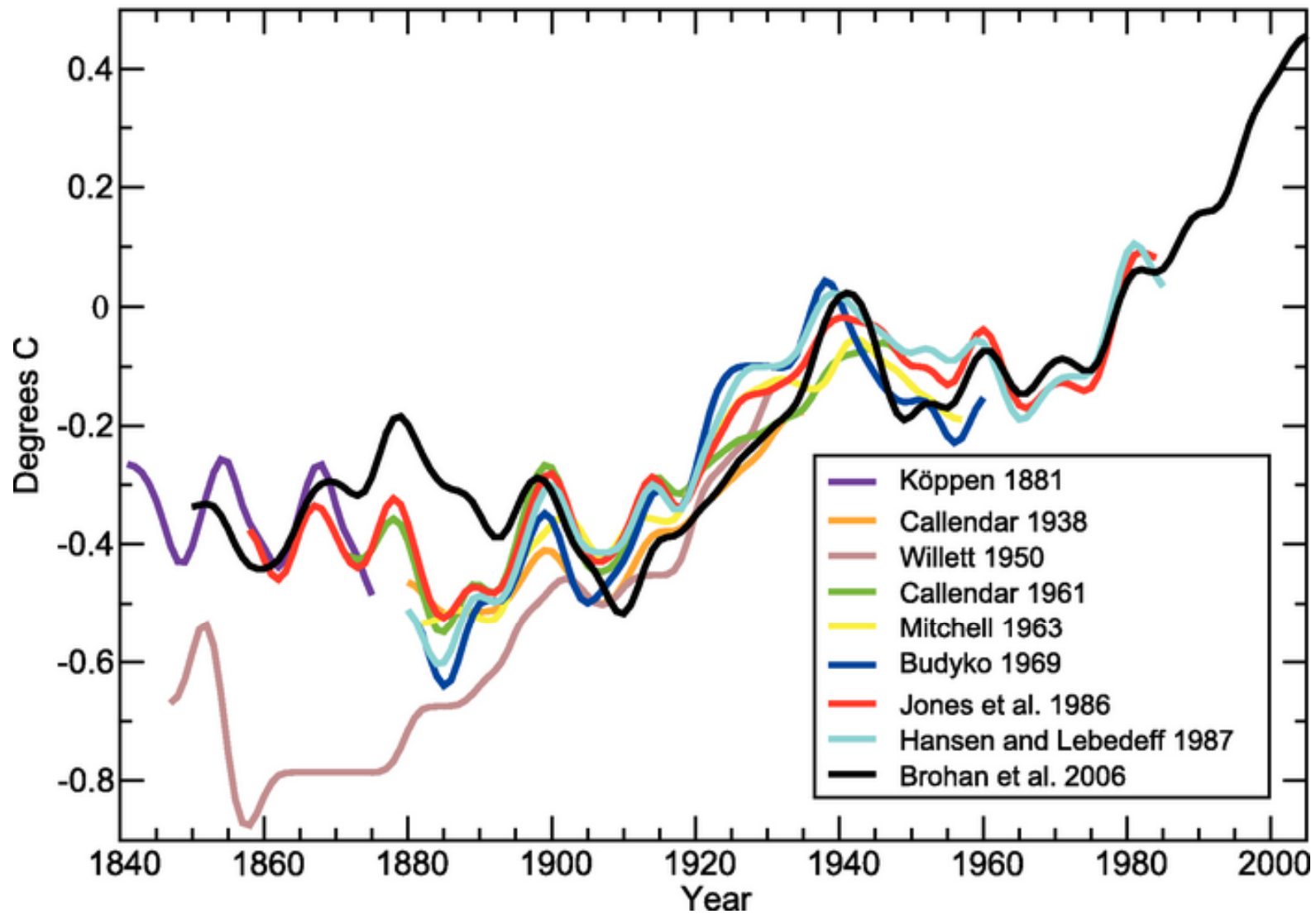


[Rock](#) has a very low [thermal conductivity](#) which means that it can take centuries for rocks underground to become aware of changes in surface temperatures. By taking very careful measurements of the temperature of [rock](#) in boreholes tens and hundreds of meters underground, it is possible to detect shifts in the long-term [mean](#) surface temperature at that location. This is underlying goal of borehole temperature reconstruction. However, as thermal [diffusion](#) is such a slow process, short term changes are averaged out and this technique only provides information about changes in the long-term average temperature. Here the borehole temperature reconstruction assigns a single rate of temperature change for each of the last five centuries and thus does not capture short-term variability.



Historical Analyses of Global Temperature

Global Temperature Time Series



Estimates of Global Mean Surface Temperature from the Instrumental Record

